

# **Flood Control in Toulmins Spring Branch Watershed through LID Practices**

by

Enis Baltaci

A thesis submitted to the Graduate Faculty of  
Auburn University  
in partial fulfillment of the  
requirements for the Degree of  
Master of Science

Auburn, Alabama  
June 15, 2016

Keywords: SWMM, LID, Flooding, Coastal watershed, Stormwater, Rain Barrel, Permeable Pavement,

Copyright 2016 by Enis Baltaci

Approved by

Latif Kalin, Chair, Professor of School of Forestry and Wildlife Sciences  
Puneet Srivastava, Professor of Biosystems Engineering  
Eve Brantley, Associate Professor of Crop, Soil, and Environmental Sciences

## Abstract

Urbanization is known to cause increases in volume of stormwater runoff and peak flow rates, which leads to changes in natural flow regime and increases the likelihood of flooding. Conventional stormwater management practices mainly focus on reducing peak flow rates; surface runoff volume reduction has traditionally been ignored. Conversely, Low Impact Development (LID) practices seek to increase infiltration to reduce runoff volume and peak flow as close to the source as possible, and are generally considered to be a more sustainable solution for urban stormwater management. In this study, the effectiveness of two LID practices, rain barrel and permeable pavements, in mitigating urban flooding was tested within the 7.95 km<sup>2</sup> Toulmins Spring Branch Watershed (TSBW) in southwest Alabama. The main motivation of studying the flooding problem in the TSBW was the frequent complains of its residents about chronic flooding. The EPA Stormwater Management Model (SWMM) was first calibrated with observed stage data at multiple sites then was used to identify the areas prone to flooding. Effectiveness of various LID practices in reducing peak flow and runoff volume at these areas were then explored with SWMM. Results indicate that LID controls can have considerable benefit for stormwater management by reducing runoff volume and peak flow rates, potentially returning watersheds to their natural flow regimes, thereby minimizing the flooding of urbanized areas. However, the effectiveness of LID controls, especially for the runoff volume, quickly diminish as the return period of the storms increase. Rain barrels were identified as the most economical and effective LID control within the TSBW drainage system.

## Acknowledgments

I would like to thank my advisor, Dr. Latif Kalin, for the SWMM program help he provided me with, for helping me navigate this Thesis project, and for making time for me in his busy schedule. I wish to thank my thesis committee members Dr. Puneet Srivastava and Dr. Eve Brantley.

I am indebted to my parents for their encouragement and blessing all through my life without whom all the achievements in my life would not have been possible. I also thank my friends for their love and support in all walks of my life.

I would like to offer my regards to Tom Herder for making the field visits enjoyable and remarkable. I want to thank Dr. Navideh Noori and Mehdi Rezaeianzadeh for their help in laboratory and office work and Dr. Ferhat Kara, Akin Un, Rasika Ramesh, Ilkim Cavus, Rajesh Sawant, City of Prichard residents, and the Mayor for their help during my field work. I also would like to recognize and thank Dr. Robin Governo for her help in the laboratory.

Lastly, I would like to thank the Turkish Ministry of Forestry and Water affairs, the Center for Environmental Studies at the Urban-Rural Interface, and the Mobile Bay National Estuary Program for the funding provided to me at various stages of my graduate study.

## Table of Contents

Abstract .....	ii
Acknowledgments.....	iii
Table of Contents.....	iv
List of Figures .....	vi
List of Tables .....	ix
List of Abbreviations .....	x
1. INTRODUCTION.....	11
1.1. Common LID Practices .....	17
1.1.1. Rain Barrels.....	17
1.1.2. Cisterns.....	17
1.1.3. Permeable Pavement .....	18
1.2. Toulmins Spring Branch.....	19
1.3. Hypotheses and Objectives.....	21
2. MATERIAL AND METHODS .....	22
2.1. Study Area .....	22
2.2. Data Collection.....	28
2.2.1. Stream data collection .....	28
2.2.2. Precipitation .....	30
2.2.3. Stream Cross sections.....	32
2.3. Model Development .....	33
2.3.1. Physical Components in SWMM.....	34
2.3.2. SWMM Settings and Inputs .....	42

2.4. LID Component in SWMM.....	46
2.5. Calibrated Strategy .....	47
2.6. Design Storms.....	48
2.7. Floodplain Maps .....	50
2.8. Flood Generating Areas.....	51
3. RESULTS .....	53
3.1. Observed Stage Levels .....	53
3.2. Model Performance .....	56
3.3. Design Storms.....	68
3.4. Floodplain Maps .....	73
3.5. Flood Generating Areas Index.....	74
3.6. SWMM LID Scenario .....	77
3.6.1. Rain Barrels and Cisterns.....	77
3.6.2. Permeable Pavements.....	78
3.7. Discussion.....	83
3.7.1. LID choice.....	83
3.7.2. Uncertainty in Rainfall Data .....	84
3.7.3. Clogged Channels .....	86
3.7.4. Junction 20 and 28 Capacity .....	87
3.7.5. Education.....	87
4. CONCLUSIONS.....	89
5. FUTURE WORK.....	92
REFERENCES .....	94

## List of Figures

Figure 1. 1: Prichard City boundaries .....	20
Figure 2.1: Location and Boundary of the Toulmins Spring Branch Watershed .....	22
Figure 2.2: Elevation map of the TSBW .....	23
Figure 2.3: Soil and Land Cover/Land Use Map of TSBW .....	24
Figure 2.4: Precipitation and temperature time series of Mobile, AL in 2015 .....	25
Figure 2.5: Two sites within the TSBW where locals complain about flooding issues at their property. See Figure 2.7 for location. ....	26
Figure 2.6: Water backed up due to the channel being clogged below the West Prichard Avenue Bridge.....	27
Figure 2.7: Locations of the flood complained areas shown in Figures 2.5 and 2.6 .....	27
Figure 2.8: Pressure transducer locations within the Toulmins Spring Branch Watershed.....	28
Figure 2.9: Installed pressure transducer using two-inch PVC pipes secured with the T-posts at site 5 .....	30
Figure 2.10: Rain gauge installed at the Prichard Municipality complex.....	32
Figure 2.11: Left picture is shown in concrete channel and right picture is shown in natural stream in TSB Watershed .....	33
Figure 2.12: TSBW water system model in SWMM with subwatersheds S1 to S36 indicated ...	35
Figure 2.13: Percent Imperviousness within the Toulmins Spring Branch Watershed .....	36
Figure 2.14: Hydrologic and hydraulic Model of TSBW by SWMM .....	41
Figure 2.15: Tide time series at the outlet point of TSBW .....	45
Figure 2.16: Conceptualization of the surface runoff SWMM LID component.....	47
Figure 2.17: Schematic representation showing the calculations of flood generating areas indices .....	52
Figure 3.1: Observed water depth at site 1 (top), site 2 (middle), and site 3 (bottom) from 9/19/2014 to 11/10/2015 .....	54
Figure 3.2: Observed water depth at site 4 (top) and site 5 (bottom) from 9/19/2014 to 11/10/2015 .....	55

Figure 3.3: Simulated/Observed water depth and Depth Duration Curve at site 5.....	58
Figure 3.4: Simulated/Observed water depth and Depth Duration Curve at site 4.....	59
Figure 3.5: Simulated/Observed water depth and Depth Duration Curve at site 3.....	60
Figure 3.6: Simulated/Observed water depth and Depth Duration Curve at site 2.....	61
Figure 3.7: Simulated/Observed water depth and Depth Duration Curve at site 1. Oscillations are tide effect .....	62
Figure 3.8: Observed and simulated maximum depths during large storms using rainfall data from both raingauge and radar at site 1 .....	65
Figure 3.9: Observed and simulated maximum depths during large storms using rainfall data from both raingauge and radar at site 2 .....	66
Figure 3.10: Observed and simulated maximum depths during large storms using rainfall data from both raingauge and radar at site 3 .....	66
Figure 3.11: Observed and simulated maximum depths during large storms using rainfall data from both raingauge and radar at site 4 .....	67
Figure 3.12: Observed and simulated maximum depths during large storms using rainfall data from both raingauge and radar at site 5 .....	67
Figure 3.13: Approximate geographic boundaries for NRCS (SCS) rainfall .....	69
Figure 3.14: 2-hour rainfall hyetograph, 5-yr return period .....	70
Figure 3.15: Overflowing junctions under a 100-yr return period storm. The coloring scheme is representative of inundation duration. Junctions shown in black indicate no inundation at all, whereas dark red junctions are exposed to longer inundation periods compared.....	72
Figure 3.16: 100- yr return period floodplain map shown on aerial photo.....	74
Figure 3.17: Flood generating areas index at junction 20 and 28.....	75
Figure 3.18: Flooded areas 5-yr return period floodplain map.....	76
Figure 3.19: Identifying and estimating the roof areas of the buildings using the city map of Prichard .....	78
Figure 3.20: Identifying and estimating the parking lot areas using the city map of Prichard....	79
Figure 3.21: Variation in peak flows under various return periods with and without LID (only rain barrel was considered) implemented at junction 20 based on subwatershed 35 .....	81
Figure 3.22: Reduction in peak flow with and without LID under different storm events at junction 28 based on subwatershed 36.....	83

Figure 3. 23. A comparison between rainfall data from radar with rain gauge data .....	86
Figure 3. 24. The channel being clogged by vegetation and trash at site 5 .....	86
Figure 3. 25. Debris along the Toulmins Spring Branch .....	88

## List of Tables

Table 1. 1: Benefits and disadvantages of LID.....	15
Table 2.1: Pressure transducer stations in the Toulmins Spring Branch Watershed .....	29
Table 2.2: Summary of subwatershed 27 properties.....	37
Table 2.3: Model Sample junction properties.....	39
Table 2.4: Sample conduit properties: c8 .....	40
Table 2.5: Sample outfall properties: Outfall-1 .....	41
Table 2.6: Green-Ampt infiltration method input parameters .....	43
Table 2.7: SWMM input parameters .....	48
Table 3.1: Observed maximum depth at each site during the period 9/19/2014 - 11/10/2015....	53
Table 3.2: The calibrated SWMM parameters.....	63
Table 3.3: Model performance statistics .....	65
Table 3.4: Estimation of time of concentration .....	68
Table 3.5: 2 hour duration storm depths for different return periods .....	69
Table 3.6: Overflowing junctions and the duration of overflows for 5, 10, 50, and 100-yr return period storms. Design storm duration is 2 hours in each, which is roughly equal to the time of concentration of the TSB watershed .....	71
Table 3.7: Reduction in peak flow, depth, and runoff volume at junction 20 based on subwatershed 34 under the use of various LIDs and with different return periods .....	79
Table 3.8: Reduction in peak flow, depth, and runoff volume at junction 20 based on subwatershed 35 under the use of various LIDs and with different return periods .....	80
Table 3.9: Reduction in peak flow, depth, and runoff volume at junction 28 based on subwatershed 36 under the use of various LIDs and with different return periods .....	82
Table 5.1. E.coli results at 5 sites.....	92
Table 5.2: The Alabama Water Watch (AWW) E.coli in water.....	93

## List of Abbreviations

Ac	Acre
CSO	Combined Sewer Overflow
DEM	Digital Elevation Model
EPA	Environmental Protection Agency
FEMA	Federal Emergency Management Agency
Ft	feet
HEC-HMS	HEC- Hydrologic Modeling Software
NAP	National academic Press
NOAA	National Oceanic and Atmospheric Administration
In	Inches
LID	Low Impact Development
LULC	Land Use and Land Cover
SWAT	Soil Water Assessment Tool
SWMM	Storm Water Management Model
TSBW	Toulmins Spring Branch Watershed
USDA	U.S. Department of Agriculture
USGS	U.S. Geological Survey

## 1. INTRODUCTION

In a natural system, floodwater spills over the channel banks and spreads over the floodplain, where it is attenuated and replenishes the groundwater. Periodic flooding provides essential services to the ecosystem. For instance, certain fish species depend on inundated floodplains for spawning. However, flooding becomes a problem when it happens in urban areas, or urban developments occur in floodplains. Floods are among the leading causes of the large natural disasters with enormous impact on humans and the environment (Siddiqui et al., 2011; Dilley et al., 2011). Floods cause billions of dollars of damage to infrastructure costing approximately \$50 billion in property damage in the 1990s alone in the United States (NAP, 2009) and property, and many human lives are lost each year to flooding (Cook and Merwade, 2009). An average of 140 people is killed by floods each year in the United States alone (USGS, 2006). From 1998 to 2007, insured flood losses totaled more than \$730 million in the United States (FEMA Fact Sheet 2008). The 2014 water year was a particularly active year for flooding; direct flood damages during the water year 2014 totaled \$2.86 billion, 36% of the thirty-year average (1984-2013) in the United States (NOAA, 2014). There were 55 flood-related fatalities, and approximately 70% of these deaths were attributed to flash flood events. Flooding is listed as the most common and frequent natural disaster in the state of Alabama as well. This is especially the case for coastal Alabama because of the low elevations and the abundance of rain. In 2005, the storm surge from Hurricane Katrina led to more than \$285 million in insured flood damage to the state of Alabama's coastal communities and, just one year prior, Hurricane Ivan caused even greater harm - more than \$355 million (FEMA Fact Sheet 2008).

In coastal regions, floods are caused by two factors: large rain events and storm surges resulting from hurricanes. Although the weather is the major driver for both types of floods, land use and cover (LULC) change (especially urbanization) can exacerbate the magnitude of floods resulting from the former cause (i.e., large storms). It is well-founded now that increased impervious surfaces, a consequence of urbanization, increases both frequency and magnitude of peak flows (Lazaro 1990, Shaw 1994, Moscrip and Montgomery 1997, Rose and Peters 2001). Urbanization results in increased flood risks and urban floods can happen in a relatively short time. Increases in the impervious surfaces associated with urbanization can result in enhanced surface runoff (Hollis 1977; Jennings and Jarnagin 2002; Waananen 1969), increased runoff velocity and reduced time of concentration (Leopold 1968).

As the population along the Alabama coast grows, it leads to land conversion mainly from rural to urban. As more forested and agricultural areas are converted to urban and suburban areas, the percentage of impervious surfaces increases and water infiltration into the soil decreases, which results in reduced time of concentration and increased surface runoff and flow rate in urbanized watersheds and eventually increase the likelihood of flooding. Increasing home sites, parking lots, buildings, and roadways can reduce area available for infiltration.

The use of Low Impact Development (LID) practices can minimize the adverse impacts of urbanization on hydrology and moderate flooding issues in urban areas (Ahiablame et al., 2013; Liao et al., 2013). LID is an environmental principle to control urban rainfall and stormwater runoff at the source. LID has been suggested as a creative solution for stormwater management (Andoh and Declerck, 1997; Montalto et al., 2007; Palhegyi, 2009; Lee et al., 2013). The LID approach is approved as an alternative to traditional stormwater design to detain,

store, infiltrate, treat urban runoff, and therefore decrease hydrological impacts of urban catchments (Dietz, 2007; Alfredo et al., 2010; Jia et al., 2012).

Consideration of LID practices for land planning is recommended since they focus on the causes instead of the symptoms of urban stormwater problems. Conventional stormwater management focuses mainly on reducing peak flow rates but makes no effort to decrease the increased runoff volume. Further, traditional practices are not able to fully restore the natural flow regime in urban streams, which can result in severe erosion of stream channel (Roesner, Bledsoe, & Brashear, 2001). However, LID practices are capable of reducing the volume of urban runoff with the reduced impervious surfaces to allow water to infiltrate to the soil (EPA, 2007). Many studies indicate that bioretention cells improve watershed hydrology and water quality (Davis et al. 2003; Dietz and Clausen 2006; Hunt et al. 2008; Davis 2008). Zahmatkesk et al. (2014) studied the potential effect of LID implementation in the Bronx River watershed in New York City under future climate change projections. They investigated LID control scenario consisting of rainwater harvesting, porous pavement, and bioretention using the SWMM model and found that peak flow rates were decreased by an average of 8 to 13%. LID practices in the watershed also reduced runoff volume equivalent to 2-year and 50-year return periods, by 28 and 14%, respectively. Lee et al. (2012) analyzed the hydrologic impact of LID practices of the rainwater management demonstration district of AsanTangjung New town in Korea using the SWMM model for preventing flooding and restore the natural hydrology. LID practices, including constructed wetlands, infiltration trenches, rain barrels, and vegetation swales were installed in this area based on land use, soil characteristic and green spaces and they found that peak flood discharge was reduced by 7 to 15% depending on the return period of the storms. Lee et al. (2013) studied the effect of LID on runoff in Cheon-an city, Korea where significant flood

damages were experienced. Three biggest flood rain events over the past 38 years were selected to examine the impact of LID techniques using the SWMM model. Results indicated that LID controls under historical storm conditions could decrease peak runoff by around 55-66% and runoff volume about 25-121% compared to that without the LID design. Liao et al. (2013) found that rain barrels as LID practice under one year return period and 60 minutes rainfall duration can reduce the waterlogging reduction (the saturation of soil with water) by about 78% for the Caohejing drainage system in Xuhui District, Shanghai, China. Rain barrels, based on their life cycle costs, are considered as suitable waterlogging reduction strategies to the drainage system. Qin et al., 2013 analyzed the impacts of LID practices of porous pavement, green roof, and swale on urban flooding and compared with the traditional stormwater design (base case) in the southwest of Guang-Ming New District, Shenzhen, China. The study area was divided in to 25 subwatersheds. 10% of the area of each subwatershed was set as swales, 80% of the area of one whole subwatershed and 20% of the other subwatershed areas were converted to porous pavements, and green roofs accounted for 20% of the area of the 22 subwatersheds. They found that all three LID scenarios were more effective for reduction of flood during heavier and shorter storm events. The swales had the best impact with an early peak, the permeable pavements had the best impact with a middle peak, and green roofs performed best with a late peak, respectively during the storm event. Abbott and Comino- Mateos (2003) analyzed the outflows collected over thirteen-month and twenty rain events, from a permeable pavement system installed in a parking lot at Wheatley, near Oxford, UK. They found that the peaks of storm events were considerably decreased as they flowed out of the porous system and on average, only 22.5% of runoff left the system during the rain event which lasted 2 hours. The surface infiltration rate of porous pavement bricks was 50 times greater than the normal bricks; however, the car park surface was

clogged by dirt and oil several times and needed cleaning. Fassman and Blackbourn (2010) studied the runoff from a small porous pavement site and an adjacent traditional asphalt site catchment in Auckland, New Zealand from 2006 to 2008. They found that the peak flow from a permeable pavement is less flashy than that from asphalt surface during storms, and they suggested that porous pavements can reduce big design storm flows, but their proper installation is a key for their proper functioning.

Table 1.1 shows the advantages and disadvantages of LID practices compared to the traditional stormwater management practices (Simpson, 2010).

**Table 1. 1: Benefits and disadvantages of LID**

Criteria	Advantage	Disadvantage	Source
Design		Harder to design than conventional storm drainage controls	(Earles, Rapp, Clary, and Lopitz, 2009)
Maintenance	Mowing and trash removal	More impressionable to maintenance than conventional stormwater management Permeable Pavements need periodic vacuuming	(EPA, 2000)
Space Requirements	Adapts in small areas Requires smaller storm drain pipes Decrease the need for a detention pond		(EPA, 2000)
Cold Climate	Performs in all climates Permeable Pavements diminish need for deicing		(Houle, 2008) (Coffman, 2009)
Constructability		More difficult than traditional stormwater management	(Ferguson, 2005)

		Improper construction causes premature failure	
Likelihood of Failure		More susceptible than conventional facilities	(Simpson, 2010)
Multi-Use	LID and Traditional BMP's can both be multi-functional amenities if designed well		(Prince George's County, 2000a)
Aesthetics	Adds to landscape value Adds amenities to landscape		(Prince George's County, 2000a) (Stahre, 2008)
Cost	Smaller storm drainage and detention system will be less costly than conventional stormwater systems	Permeable Pavements have higher upfront costs	(Prince George's County, 2000a) (EPA, 2007)
Peak Flow Rate Reduction	Can be achieved if designed properly		(Prince George's County, 2000b) (Lee, 2012) (Zahmatkesk, 2014)
Flow Duration Reduction	Can diminish flow duration		(Prince George's County, 2000a)
Volume reduction	Potentially significant reductions under the right conditions		(Prince George's County, 2000b) (Lee, 2012) (Zahmatkesk, 2014)
Ground Water	Depends on soils		(Prince

Recharge/ Stream Base Flow	Potentially very high		George's County, 2000a) (Ferguson, 2005)
Regulation		Rely on region Discrepancy in regulations between entities	(Earles, et al., 2009)

Adapted from Simpson (2010)

## 1.1. COMMON LID PRACTICES

### 1.1.1. Rain Barrels

Rain barrels are residential cost effective, easily maintainable retention and detention devices, that capture and store the rainwater that falls on the rooftop so that runoff from impervious surfaces can be reduced. Roof systems typically collect rainwater through a connection to a rain gutter system. A typical rain barrel design has a hole at the top to allow stormwater to flow from a downspout, a sealed lid, an outlet for excess water (overflow pipe) and a faucet at the bottom of the barrel. The faucet can be partially opened to detain water or closed to fill the barrel. The water can then be used for watering a lawn and garden or other uses such as flushing toilet. Rain barrels can also help decrease homeowner's water bill when they are used for watering the garden during the hot summer months.

### 1.1.2. Cisterns

Cisterns are larger storage tanks that provide retention storage volume in above or underground for commercial or agricultural settings. They are typically used when large volumes of water

need to be collected. Cisterns are larger than rain barrels, with some underground cisterns having the capacity greater than 10,000 gallons. The collected water in a cistern can be used for irrigation, vehicle washing, and laundry.

Using large storage systems such as rain barrels or cisterns is not a new technology and practice as harvesting rainwater (Ahiablame et al., 2013). These practices have been in use for several thousand years in Europe, Asia, Africa, Middle East, and South America, where the stormwater is collected by rain barrels and cisterns for agricultural activities, drinking water, and touristic purposes (Roebuck, 2007; Leung, 2008). Research indicate that stormwater runoff can be controlled by harvesting rainwater with appropriate tank sizes (Aad et al., 2010; Damodaram et al., 2010), and they can provide minimum 50% of the nonpotable water need for human uses such as flushing toilet, garden irrigation, and washing machines (Roebuck, 2007). The interest in rainwater harvesting has recently increased as an approach to optimize the use of available water sources due to climate change and drought effects (Pandey et al., 2003; Kaspersen, 2012). Cisterns are effective and easily maintainable retention and detention devices that are applicable to urban areas (Aad et al. 2010; Damodaram et al. 2010).

### **1.1.3. Permeable Pavement**

Paved roads and parking lots occupy large areas in developed areas, which play a significant role in transporting stormwater runoff and contaminant loads to receiving waters. Alternative paving materials can be used to infiltrate stormwater locally and diminish the runoff leaving a site. This can help reduce downstream flooding and the frequency of combined sewer overflow (CSO) events. Use of these materials can also remove problems with waterlogging, supply for groundwater recharge, help control erosion of stream beds and river banks, and provide for a

more aesthetically pleasing site (Pratt et al., 1999; Scholz and Grabowiecki, 2007). Through use of permeable pavement, the effective imperviousness of any given project is reduced while land use is maximized. The drainage of paved areas and traffic surfaces by means of permeable systems is an important building block within an overall LID scheme that seeks to achieve a stormwater management system close to natural conditions.

Studies in the literature indicated a considerable reduction in the surface runoff that leaves a porous paver site due to increased infiltration rate. For instance, in the University of Guelph experiments, study sites with permeable concrete pavers had a 90% reduction in runoff volume (James, 2002). However, this decrease may be insignificant at subwatershed level. Research has shown that permeable pavement systems have comparatively lower infiltration rates than soils (Dreelin et al., 2006), yet still reduce runoff and enhance water quality (Scholz and Grabowiecki, 2007; Dietz, 2007; Ahiablame et al., 2012a). Although porous pavements can be considered as a LID source control and can reduce conventional large design storm flows as well, their proper installation and maintenance is a key for their proper functioning (Fasman and Blackbourn, 2010).

## **1.2. Toulmins Spring Branch**

The underserved residents of the Toulmins Spring Branch (TSB) community (Figure 1.1), north of the city of Mobile, have been complaining that even 25 mm rain sometimes floods their backyard and sometimes their home based on the information provided from the Mobile Bay National Estuary Program (MBNEP) and personal communication. The TSB watershed (TSBW) is susceptible to flooding due to (i) low elevation, (ii) abundance of heavy rains, (iii) high

impervious cover, and (iv) potential sea level rise and increased storm surge. Mobile County also had similar complaints; they have spent millions of dollars for infrastructure repair every year due to frequent floods (MBNEP and personal communication). Therefore, there is a need for identifying the main causes of flooding experienced by locals of TSB community and identification of target areas for increased stormwater management and intensive education of public works personnel related to LID practices that can aid in reducing flooding impacts.



**Figure 1. 1: Prichard City boundaries**

While LID practices can efficiently manage stormwater and improve the post-development flow regime for small design events, the budget restriction might not allow retrofitting all existing parking spaces or rooftops in a watershed with these methods. Some areas in a watershed may be vital for decreasing stormwater, and effective watershed management should identify these locations where LIDs should be implemented to best mitigate the peak flow and improve the hydrologic sustainability of the watershed while minimizing costs. This research focuses on simulating the hydrologic behavior of LID practices in the TSB watershed. The LID practices, including rain barrels and permeable pavements, were considered to investigate the impact of

LIDs on the TSB streamflow. Rain barrels and permeable pavements were selected based on cost-effectiveness and the area available for LID. These LID controls were simulated using the Storm Water Management Model (SWMM) to facilitate watershed management in TSBW.

### **1.3. Hypotheses and Objectives**

The main ***hypothesis*** of this project is:

*“Areas that contribute to downstream flooding can be identified through the development of a hydrologic/hydraulic model and by incorporating Low Impact Development practices in these hydrologically sensitive areas, downstream flooding can be mitigated effectively.”*

The specific objectives are:

- i. Determine whether flooding in the Toulmins Spring Branch watershed is due to lack of maintenance or inadequate infrastructure for drainage of storm water:*

This was achieved by combining stage data with field visit observations.

- ii. Assess the utility of various LID practices in flood generating areas in order to mitigate downstream flooding.* The LID practices to be tested include rain barrels and permeable pavements.

## 2. MATERIAL AND METHODS

### 2.1. Study Area

The Toulmins Spring Branch Watershed ( $7.95 \text{ km}^2$ ) is a sub-watershed of the Three Mile Creek watershed in Mobile County, Alabama. Part of the watershed is located within the Mobile city limits and the rest is within the city of Prichard (Figure 2.1). Surface runoff generated by the TSBW flows into Three Mile Creek, which flows into Mobile Bay and eventually to the Gulf of Mexico. The TSBW is approximately 2 km long in an east-west direction and 5 km wide in a north-south direction. The maximum elevation of the watershed is 20 m and the minimum elevation is about -1 m as shown in Figure 2.2. Average slope of the watershed is 1.75%.

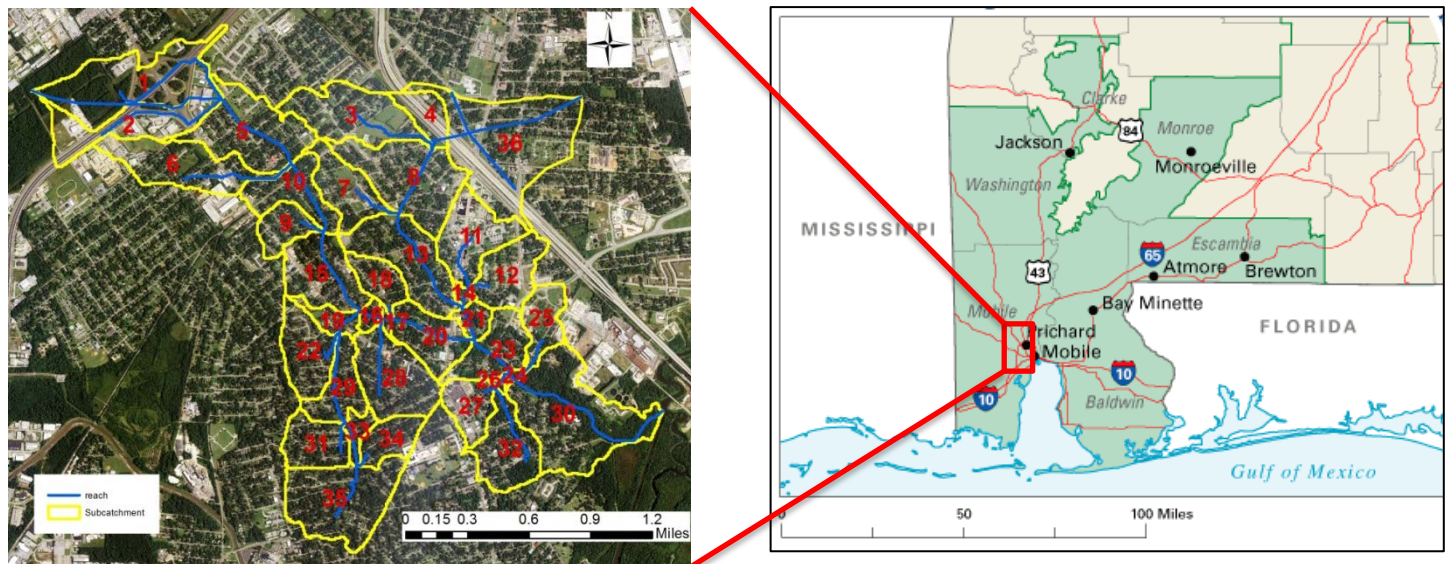


**Figure 2.1: Location and Boundary of the Toulmins Spring Branch Watershed**

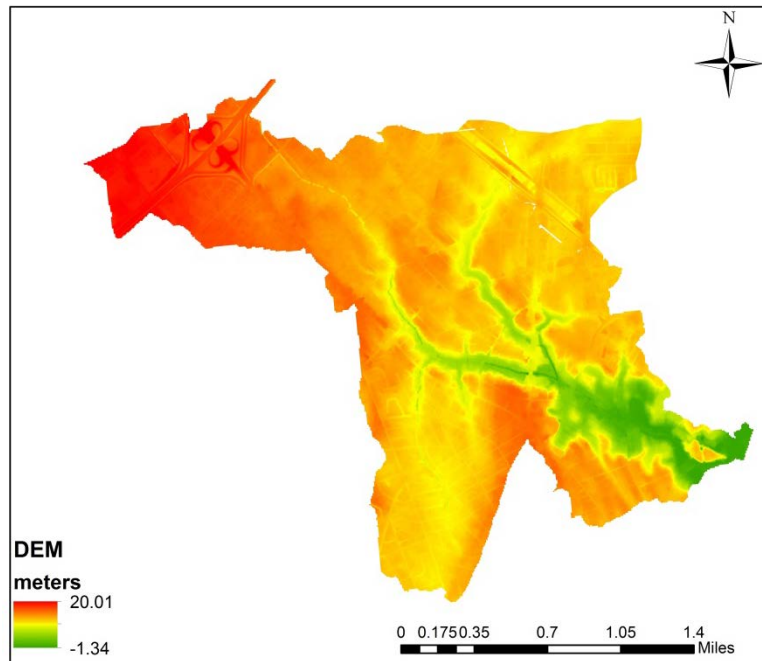


**Figure 2.2: Elevation map of the TSBW**

Soil types within the study area include Benndale sandy loam (~41%), Harleston sandy loam (~28%), and Smithon sandy loam (~17%), with the additional 14% made up of miscellaneous soil types as shown in Figure 2.3. The 2011 NLCD Land Use/Land Cover map (Figure 2.3) lists the study area as 93% developed, 6% is wetlands, and 1% is forest and shrub.

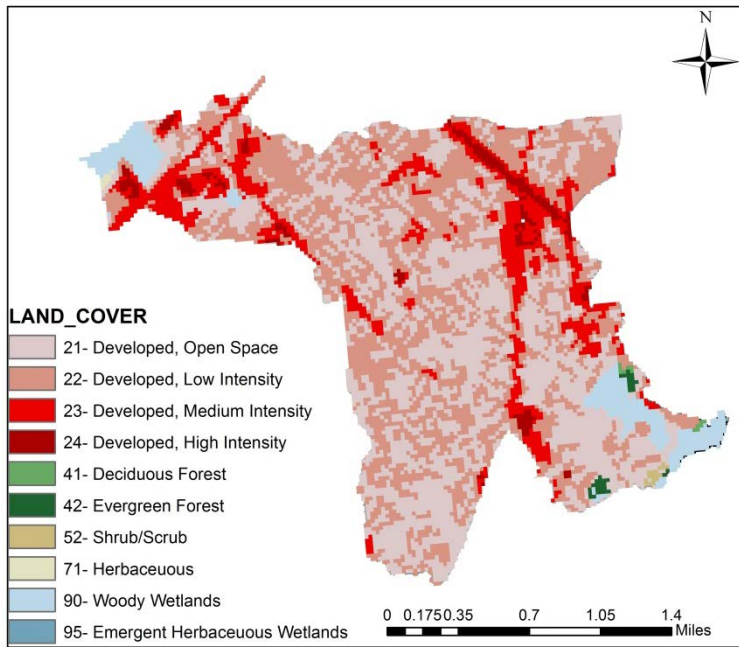
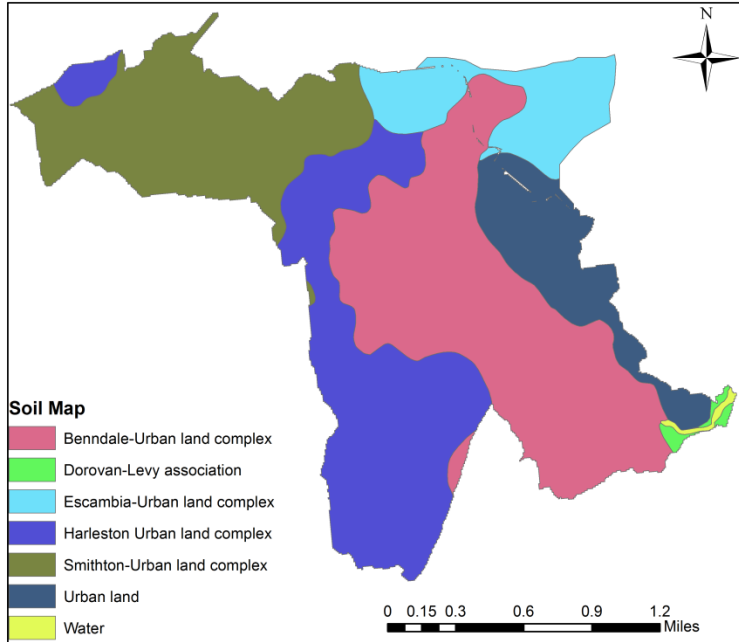


**Figure 2.3: Soil and Land Cover/Land Use Map of TSBW**

In 2015, which covered most of the study period, the contiguous United States (CONUS) average precipitation was 876.3 mm, 115.6 mm above the 20<sup>th</sup> century average. However,

Mobile, AL received 2065 mm rain in 2015 which is more than double the U. S. average rainfall and approximately 380 mm above average for Mobile, AL as shown in Figure 2.4 (NOAA, 2016).

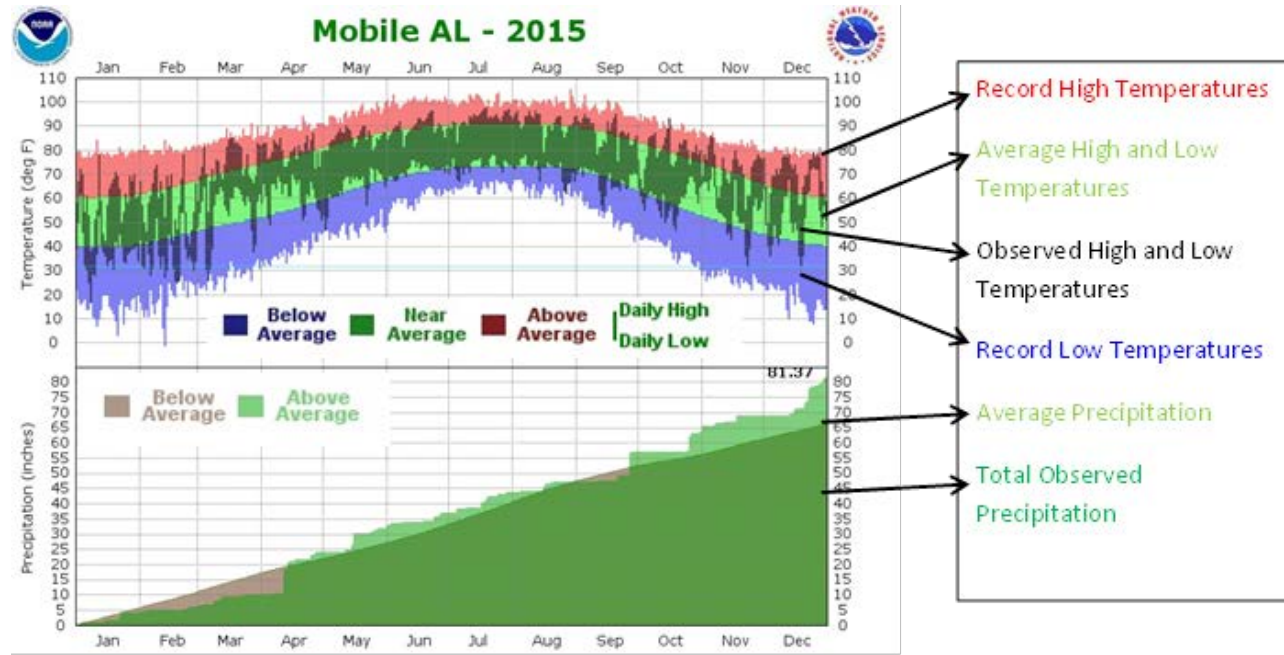


**Figure 2.4: Precipitation and temperature time series of Mobile, AL in 2015**

According to estimates prepared by the U.S. Bureau of the Census, Prichard's population was 22,659 in 2010, down from a reported population of 27,963 people in 2005, and annual per capita income was \$12,433 in 2014. The percentage of residents in Prichard who live below the poverty level is 35.4%. As a result, infrastructure and personal properties are often not well maintained.

Within the city of Prichard, two locations were identified where residents reported regular flooding on their property (Figure 2.5). On Chastang Avenue, we interviewed a local resident (left picture), and he said water gets up to the plinth level of his house and causes damage to his properties. The right side of Figure 2.5 shows a home on the Josephine Street that gets flooded by the creek. The owner of this home also complained that a drainage pipe ends

right in front of his house, resulting in stormwater from other areas being discharged to his property, causing damage and inconvenience for him regularly. We also observed waterways clogged by debris at multiple sites, potentially contributing to flooding (Figure 2.6). Figure 2.7 indicates these reported areas on the map.



**Figure 2.5:** Two sites within the TSBW where locals complain about flooding issues at their property. See Figure 2.7 for location.



**Figure 2.6: Water backed up due to the channel being clogged below the West Prichard Avenue Bridge**



**Figure 2.7: Locations of the flood complained areas shown in Figures 2.5 and 2.6**

## 2.2. Data Collection

### 2.2.1. Stream data collection

Water depth (stage) was continuously monitored at 5 sites. Limited flow measurements were also taken. Water level (pressure) transducers were installed and placed at five locations on October 14<sup>th</sup> 2014 (Figure 2.8). Monitoring continued until November 10<sup>th</sup> 2015. Model 3001 Levelogger Edge was used for this purpose, which is a self-contained water level datalogger. The data from the levelogger can be retrieved using any laptop with the required software. The Levelogger Edge has a memory capacity of 40,000 temperature and water level data points (Solinst, 2016). The pressure transducers were set to record water levels ( $h$ ) at 15 minute intervals. The data was retrieved during site visits after significant rain events. Table 2.1 describes the locations of the pressure transducers within the TSB watershed.

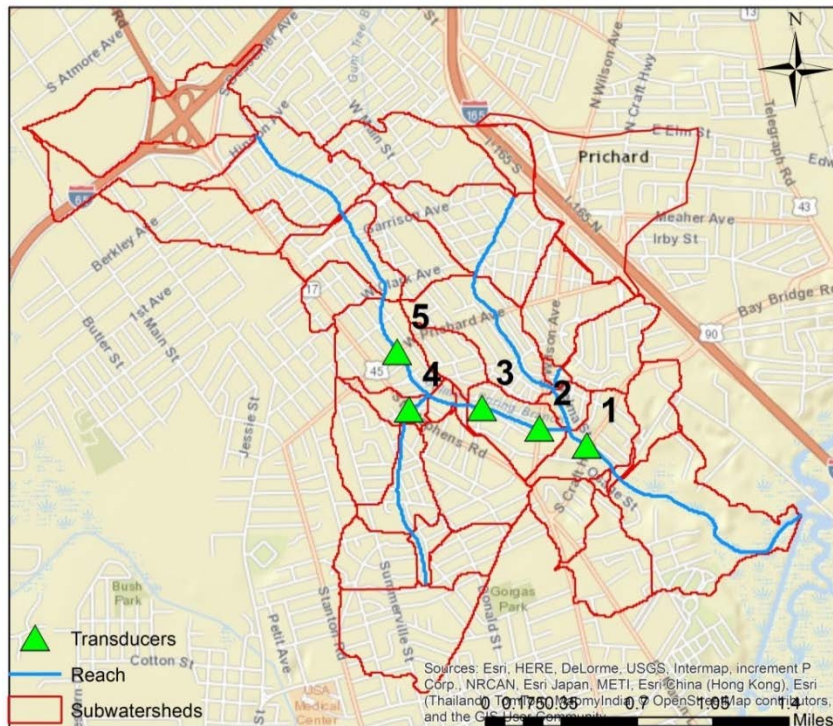


**Figure 2.8: Pressure transducer locations within the Toulmins Spring Branch Watershed**

**Table 2.1: Pressure transducer stations in the Toulmins Spring Branch Watershed**

<b>Station ID</b>	<b>Station Description</b>	<b>Latitude</b>	<b>Longitude</b>
1	At S Craft Hwy	30.721695	-88.080457
2	At S Wilson Ave	30.722993	-88.083428
3	At Sweeneys Ln	30.723989	-88.087353
4	At Toulmin Ct	30.723264	-88.093094
5	At W Prichard Ave	30.727012	-88.093094

As shown in Figure 2.9 the pressure transducer units were installed using 5 cm PVC pipes as an outer casing to protect them. The PVC pipe is secured with a T-posts. The pipes have several holes at the bottom where the loggers are resting so water can flow through. A smaller hole can be drilled near the top of the pipe to allow for air movement when the water levels fluctuate. The 5 cm well caps fit snugly on the top end of the PVC pipes. The end of the cable that connects to the logger slides through the opening of the well cap, which leaves the direct-reading end out in the open. Therefore, the leveloader can be connected whenever the reading is needed.



**Figure 2.9: Installed pressure transducer using two-inch PVC pipes secured with the T-posts at site 5**

Three discharge measurements were taken because water levels were very low during site visits and most significant rain events generally happened at midnight. Flow was measured with Acoustic Doppler Current Profiler (ADCP). On 01/23/2015, the discharge measurement was taken at sites 1, 2, 4, and 5 only. Because of the extremely low flow, the discharge measurement could not be taken at site 3 on that day. On 02/25/2015 and 03/15/2015 the discharge measurement was taken at sites 1, 2, and 5 only.

### **2.2.2. Precipitation**

Rainfall data in this study comes from a 15 cm tipping bucket rain gauge along with the Solinst Rainlogger, which was deployed at the Prichard Municipality complex (Figure 2.10). The gauge

has been in operation since 10/14/ 2014. In addition to the rain gauge, rainfall data from several other sources were also considered. One source for precipitation data was the Community Collaborative Rain, Hail & Snow Network (CoCoRaHS) station (# AL-MB-4 and # Mobile 2.6 WNW), which is located southwest of the TSB watershed. Data from Center for Hurricane Intensity and Landfall Investigation (CHILI) in Mobile (USA Campus West) station (Latitude: 30.6944°N, Longitude: 88.1944°W) was used as well. Radar-based rainfall data obtained from State Climate Office of North Carolina was also used. The precipitation data obtained from all these stations were evaluated when the SWMM model was being calibrated. Rainfall data from all stations, when compared to the rain gauge deployed at the Prichard Municipality, indicated a high variability in precipitation through the TSB watershed. The gauge data had a better correspondence with measured stage data, and therefore was the choice as precipitation data source. Further, because of the small size and the flashy character of the watershed high temporal resolution precipitation was needed. Radar is useful but does not provide data below 1 hour temporal resolution. The temporal scale ( $dt$ ) of rainfall data in this study was 15 minute. Sensitivity analysis showed that model results do not change much when  $dt$  was less than 15 minute. The rain gauge in the study area records every minute, but can provide output at any time interval.



**Figure 2.10: Rain gauge installed at the Prichard Municipality complex**

Temperature data was obtained from the Center for Hurricane Intensity and Landfall Investigation (CHILI) and was imported into the model as an external climate file. Hargreaves equation was used to calculate potential evapotranspiration.

### **2.2.3. Stream Cross sections**

A survey rod and level were used to measure the channel cross-section where it changes along the stream during the field visit. Most of the TSBW is channelized with concrete canals; only the downstream section is natural condition (see Figure 2.7). Figure 2.11 shows examples of a concrete channel and a natural channel from the watershed.



**Figure 2.11: Left picture is shown in concrete channel and right picture is shown in natural stream in TSB Watershed**

### 2.3. Model Development

In this study, the Environmental Protection Agency Storm Water Management System (EPA SWMM) was used to model the streamflow and flow depth within the TSBW. The LID component of the model was later used to evaluate the rain barrels and permeable pavements for their potential in flood mitigation at the TSBW. Floodplain maps were generated for different return period events to identify the areas sensitive to flooding in the watershed. The calibrated SWMM model was used to estimate peak flows for various return period storms.

The SWMM model is a dynamic rainfall-runoff simulation model used for single event or long-term simulation of runoff quantity and quality from primarily urban areas. The runoff component of SWMM operates on a collection of subwatershed areas that receive precipitation and generate runoff and pollutant loads. The routing portion of SWMM transports this runoff through a system of pipes, channels, storage/treatment devices, pumps, and regulators. SWMM tracks the quantity and quality of runoff generated within each subwatershed, pipe and channel

during a simulation period. Four functional program blocks comprise the model: Runoff, Transport, Extran, and Storage/Treatment. The blocks can be overlaid and run sequentially or separately with interfacing data files. The Runoff blocks simulate the continuous runoff hydrograph and pollutograph for each subwatershed in the drainage basin. In the Runoff block, each subwatershed surface is treated as a nonlinear reservoir with a single inflow. Surface runoff is calculated using the nonlinear storage equation, which is a combination of continuity equation and Manning's equation. In addition to modeling the generation and transport of runoff flows, SWMM also estimates the production of pollutant loads from land uses during storm events and routing of water quality constituents through the drainage system.

In the following sections, SWMM ability of simulating water systems is discussed.

### **2.3.1. Physical Components in SWMM**

In SWMM, the study area's water system can be modeled as a set of physical components. Some of the physical components in SWMM include (i) *subcatchments*, (ii) *junctions*, (iii) *conduits*, and (v) *outfalls*.

#### **2.3.1.1. Subcatchments**

To obtain results in SWMM, the study area should be divided into smaller spatial subareas, each of them provided with specific properties. SWMM does not have a Geographic Information System (GIS)-based Graphical User Interface (GUI) that can delineate the subwatersheds and extract all relevant properties. ArcSWAT model was used as a pre-processor to calculate some hydrological components (Neitsch et al., 2011). Using ArcSWAT 10.1, the TSB watershed boundary and its subwatersheds were delineated using a 10 m Digital Elevation Model (DEM)

obtained from Alabamaview (Alabamaview, 2015). The study area was divided into 36 subcatchments, labeled from “S1” to “S36” as shown in Figure 2.12.

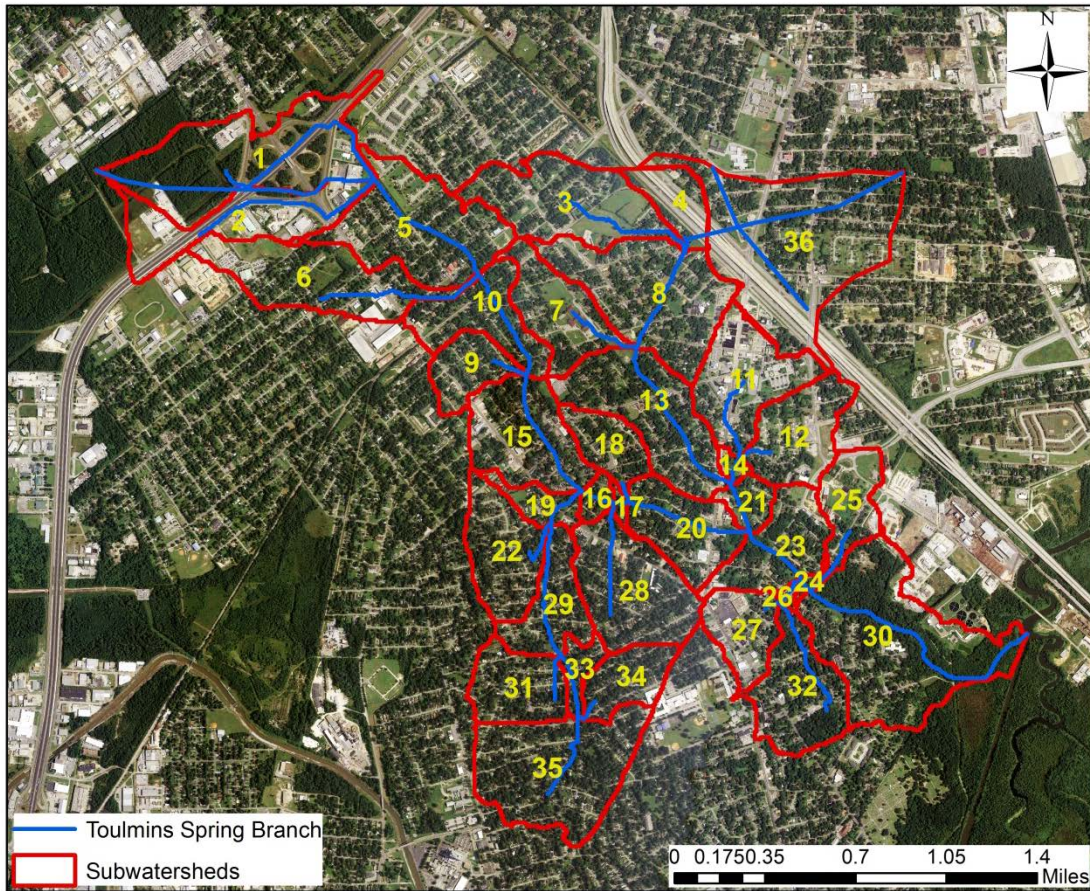


**Figure 2.12: TSBW water system model in SWMM with subwatersheds S1 to S36 indicated**

2013 aerial photography at 1 m resolution was used to estimate the imperviousness of each subwatershed using the Geographic Object-Based Image Analysis using the eCognition (GeOBIA) software. On average, 36.4% of surfaces within the TSB watershed are impervious (e.g., concrete, asphalt, roofs). Within subwatershed number 27, in particular, 62.3% of surfaces are impervious, which is the highest percentage in the study area. Properties of Subcatchment 27 are summarized in Table 2.2 which has the highest percentage of imperviousness. Conversely,

the outlet subwatershed (number 30) is the least developed, where 15.6% of surfaces are impervious. Figure 2.13 shows the distribution of imperviousness within the TSBW.

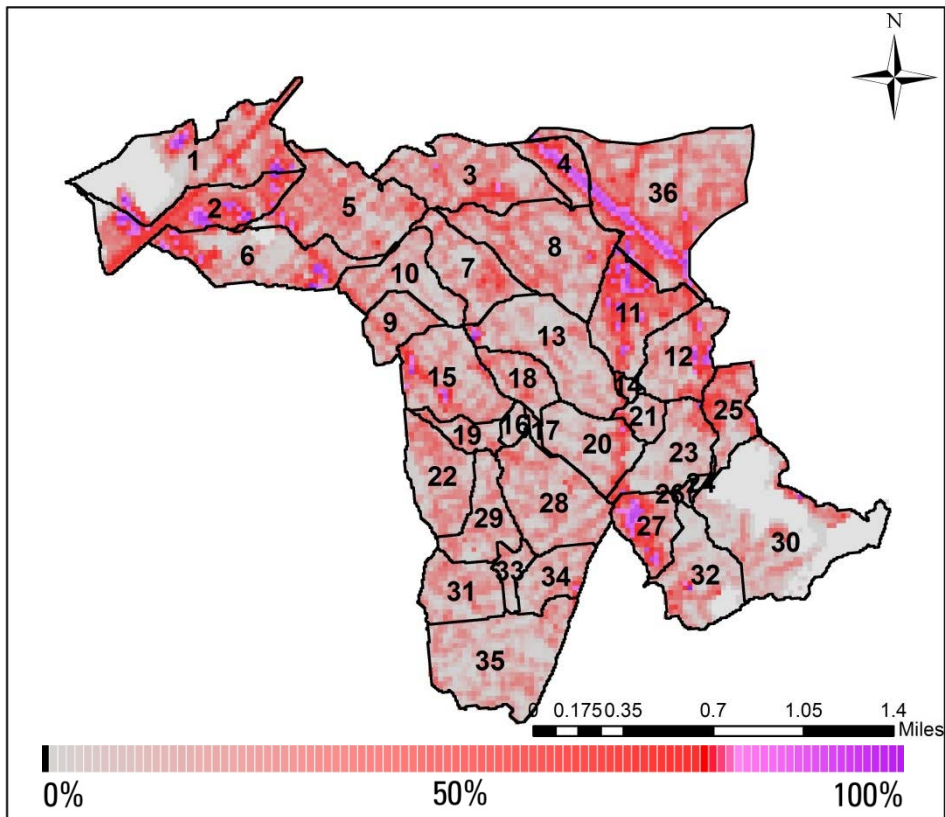


**Figure 2.13: Percent Imperviousness within the Toulmins Spring Branch Watershed**

SWMM requires each of the subwatersheds receive precipitation from a “RainGauge”. Since the research area is less than 8 km, the rainfall is assumed to be more or less uniform. Thus, only one rain gauge was used for the whole area in the model. Sensitivity analyzes showed that precipitation data at 15 minute temporal resolution was the optimal Δt for the TSBW.

**Table 2.2: Summary of subwatershed 27 properties**

<b>Property</b>	<b>Value</b>
Name	S27
Rain gage	RainGauge
Outlet	J12
Area	15.5 ha
Width	291.8 m
% Slope	3.1 %
% Impervious	62.3 %

After drawing the physical components on the study area map in SWWM, the next step is to edit the properties for the component and provide related data for each component. Generally, subcatchments are divided into 2 subareas in SWMM applications, pervious and impervious areas. Runoff can penetrate the upper soil part of the pervious subarea, but this is not the case for the impervious area. Impervious areas mostly include parking lots and asphalt roads that lead water directly to the linked junction as runoff (Rossman, 2010).

For each subcatchment area, the percentage of impervious area, i.e., the subarea in which water cannot penetrate into, and the name of the labeled junction which receives the runoff from the subcatchment are included in the subcatchment properties window. Finally, a rain gauge can also be assigned to the subcatchment properties window that directs precipitation to the catchment.

#### **2.3.1.1.1. Area, Width, & Slope**

The subwatershed area divided by the average maximum overland flow length gives an initial estimate of the characteristic width of the subwatershed. The maximum overland flow length is the length of the flow path from the outlet to the furthest drainage point of the subcatchment.

Maximum lengths from several different possible flow paths should be averaged (SWMM Manual). The slope, area, and width of each subcatchments area were calculated in ArcSWAT based on the subwatershed delineations, and was used as input for SWMM.

### **2.3.1.2. Junctions (Nodes)**

Junctions are physical components in SWMM that are drainage system nodes where links join together. Physically they can assemble the confluence of natural surface channels and pipe connections. Runoff from subwatersheds can enter the system at junctions. Excess water at a node can become partially pressurized while connecting links are surcharged, and this excess water can either be lost from the system or be allowed to pond atop the node and subsequently drain back into the node (Rossman, 2015). Elevation of junction's "invert", the decreased level of the inside of the conduit, maximum depth of the manhole, initial depth of water present in the system, surcharge depth, and ponded area are the most crucial input parameters for a junction. The distance from invert to the ground surface is the maximum water depth. If zero is used, then the distance from invert to the top of the highest connecting conduit will be used (Rossman, 2015). A storage area around the junction is the ponded area, which can store excess water and overflows the system and is lost. Ponded area is an option for re-introducing the excess area to the system as the capacity of the system (Rossman, 2015).

The main channels, which collect the overland flow from the subcatchments, were identified with ArcSWAT. These channels were introduced into SWMM as conduits. Within the SWMM, each conduit is connected with junctions, which varied depending on invert elevation and maximum depth. A total of 25 junctions were defined, one of which was the outlet point to the Three Mile Creek. For the junction's elevation, two sets of data were considered in this research. The first set was generated from 0.6 m contour map of the city of Prichard obtained

from the City of Mobile GIS department. The second set were taken by a handheld GPS. Both sets were compared and used to create elevations for each junction in the TSBW. Table 2.3 shows example data for junction 12.

**Table 2.3: Model Sample junction properties**

Property	Value
Name	J12
Invert El.	1.2 m
Max. Depth	0 m
Initial Depth	0.9 m
Surcharge Depth	0 m
Ponded Area	0

### **2.3.1.3. Conduits (Links)**

Conduits are units transferring water from one junction to another through pipes or channels. Inlet and outlet junctions, shape, length and a maximum depth of the conduit are the most vital properties of a conduit. Conduit cross-sectional shapes are entered from a variety of standard open and closed geometries as well as irregular natural cross-section properties as user-defined closed shapes in SWMM. Maximum depth of the cross-section can be considered as the diameter of the conduit in the system.

The main channels were defined with ArcSWAT and these channels were introduced into SWMM as conduits. The input parameters used for the 25 conduits included: length, cross-sectional area, roughness, and inlet-outlet node. Table 2.4 shows conduit c8's properties as an example.

**Table 2.4: Sample conduit properties: c8**

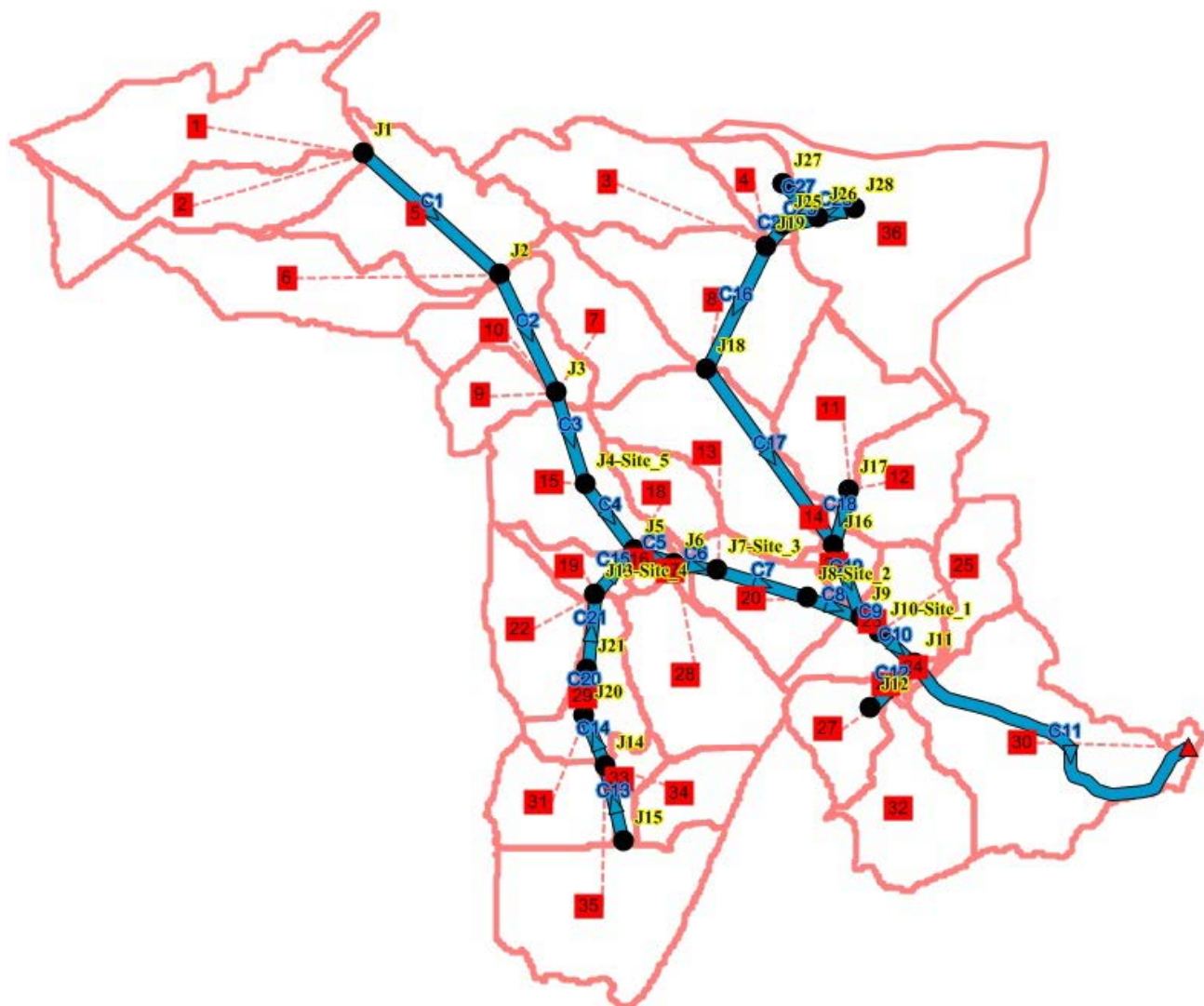
<b>Property</b>	<b>Value</b>
Name	c8
Inlet Node	j8
Outlet	j9
Shape	TRAPEZOIDAL
Max. Depth	4.6 m
Length	155.3 m
Roughness	0.012

### 2.3.1.4. Outfalls

An outfall in SWMM is a type of junction that discharges wastewater into the environment. The watershed outlet is also denoted as an outfall in the SWMM. The dynamic wave flow routing method is used in Toulmins Spring Branch Watershed which is later discussed in section 2.3.2.1 below. Each outfall can only have one conduit to be connected to it as the outflow junction for the conduit. Outfalls have specific characteristics which can be described by defining related parameters such as invert elevation, an existence of a flap gate to prevent backflow, and tidal data for tidal outfall. An example outfall data is shown in Table 2.5. Only one outfall was defined for the TSBW which is the outlet point to the Three Mile creek. Because this outfall is the connection to the Gulf of Mexico, it is exposed to the tidal effects. Therefore, the outlet was also defined as a tidal outfall. Hydrologic/Hydraulic model of TSBW by SWMM is shown in Figure 2.14.

**Table 2.5: Sample outfall properties: Outfall-1**

Property	Value
Name	Outfall-1
Inflows	NO
Treatment	NO
Invert elevation	0.2 m
Tide gate	NO
Type	TIMESERIES
Series Name	Tidal-date

**Figure 2.14: Hydrologic and hydraulic Model of TSBW by SWMM**

### 2.3.2. SWMM Settings and Inputs

In the SWMM simulation option section, general settings, dates and time steps settings need to be determined. In the general settings part, (i) different flow routing options, (ii) precipitation, and (iii) tidal flow routing are also required to be defined. Infiltration models are other choices in this section. SWMM offers mainly three infiltration options to model which are Horton equation, Green-Ampt method and the Curve Number method. The Horton equation reduces infiltration exponentially to a minimum rate during a big precipitation event from an initial maximum value. The maximum and minimum infiltration rates, a decay coefficient, and the time it takes a fully saturated soil to dry completely are required as input parameters for Horton Method. A Green-Ampt method for modeling infiltration considers a wetting front in the soil in which an initial moisture soil is separated from the saturated soil above. The initial moisture deficit of the soil, the soil's hydraulic conductivity, and the suction head at the wetting front are required as Green-Ampt input parameters. The third method is adapted from the Natural Resources Conservation Service (SCS) Curve Number method for estimating runoff based on its curve number and total infiltration capacity. The curve number and the time it takes a fully saturated soil to dry completely are the input parameters for this approach. The Green-Ampt method for modeling infiltration was selected for modeling TSBW. Relevant soil data for this method was obtained from the USDA Natural Resources Conservation Service website: <http://websoilsurvey.sc.egov.usda.gov/>. Table 2.6 shows the input parameters for Green-ampt infiltration model for a sandy loam soil. All the soils shown on Figure 2.3 have the sandy loam soil texture.

**Table 2.6: Green-Ampt infiltration method input parameters**

<b>Property</b>	<b>Value</b>
Suction Head	109.9 mm
Conductivity	14.48 mm/hr
Initial Deficit	0.263

The model is run from 09/19/2014 to 11/10/2015. 15-minutes interval was selected for reporting of computed results, and 30 seconds was the time step calculations.

### 2.3.2.1. Flow Routing

Flow routing is another key section of the general settings in SWMM. Flow routing within a channel in SWMM is governed by the conservation of mass and momentum equations for an unsteady flow. SWMM offers three ways to solve these equations for flow routing. The first routing type is steady flow routing which represents the simplest method to solve the equation. It assumes that at each time step flow is uniform and steady. Therefore, it simply translates inflow hydrographs at the upstream end of the conduit flows to the downstream end without any delay or change in shape. Steady flow routing cannot deal with channel storage, backflow effects, entrance/exit losses, flow reversal, and pressurized flow. This method is only appropriate for preliminary analysis with long-term continuous simulations in SWMM (Rossman, 2015).

The second one is the kinematic wave routing. This approach solves the continuity equations along with a simplified form of the momentum equation in each conduit. The slope of the water surface equals the slope of the conduit in this approach. The maximum flow that can be transferred through the channel is the full normal flow value. If there is overflowing in the inlet node, this excess water is either lost from the system or can have a waterlogging atop the inlet node. This approach allows flow and area to vary both spatially and temporally within a conduit.

However, this form of routing cannot deal with backwater effects, entrance or exit losses, and reverse flow. Numerical stability with moderately large time steps can usually be maintained with this method. Thus, kinematic wave method can be an accurate and efficient routing approach, especially for long-term simulations (Rossman, 2015).

The third method is the dynamic wave routing. It represents the complete one-dimensional Saint Venant flow equations. Thus, it provides the most theoretically accurate results. With this approach, flows can exceed the full normal flow value. When the water level is greater than the maximum channel depth, flooding happens. Unlike the other two methods, dynamic wave routing can be used for channel storage, backwater, entrance/exit losses, flow reversal and pressurized flow, which is the situation in this study for the Toulmins Spring Branch Watershed.

### **2.3.2.1. Tidal Flow**

Pump, storage, control, diversion, rating, shape and tidal curves are defined in the curve section in SWMM. The most vital curve for the TSB watershed model is the tidal curve, which can be defined as hourly time series for tidal levels. The consequence of the response of the ocean basin to the tide-producing forces, to the variations of tides because of the shallow water effects of local rivers, or to the regional effects of weather change on water levels can cause tides. Tides can be high or low. The horizontal flow of water toward the area with maximum solar and lunar attractions produces a high tide. A compensating withdrawal of water produces a low tide. The alternation of these two kinds of tides is the result of daily rotation of the Earth (International Hydrographic Bureau, 2005). Backflow effect can be one of the most significant effects of tides in the water system. Therefore, tidal effect is explored to this research and Tide time series downloaded from National Oceanic and Atmospheric Administration's (NOAA) Center for

Operational Oceanographic Products and Services website: <http://tidesandcurrents.noaa.gov/> for the outlet point of the TSBW is shown in Figure 2.15.

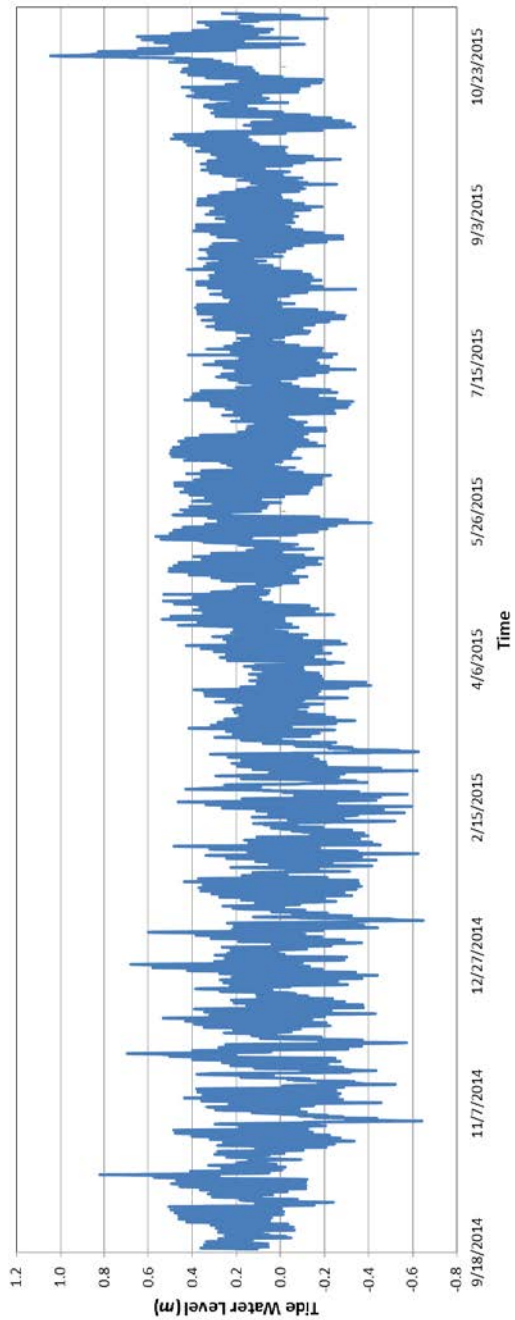


**Figure 2.15: Tide time series at the outlet point of TSBW**

## 2.4. LID COMPONENT IN SWMM

LID practices are low impact development controls designed to capture surface runoff and to store, infiltrate, and evapotranspire. They are considered as properties of a given subwatershed in SWMM. Two generic types of LID controls are explicitly modeled in this research.

1. Rain Barrels or Cisterns are storage tanks that collect runoff from a rooftop during rainfall events and can either release or allow reuse of the rainwater during dry periods (Rossman, 2015).
2. Continuous permeable pavement systems generally have a subbase of gravel and surface of porous concrete, asphalt mix or pavers. All rainfall will directly percolate through the pavement into the gravel storage layer below it where it can infiltrate at natural rates into the site's native soil. Block Paver systems consist of impervious paver blocks placed on sand or pea gravel bed with a gravel storage layer below. Rainfall is captured in open spaces between the blocks and conveyed to the storage zone and native soil below (Rossman, 2015).

Permeable pavement systems can transfer the captured runoff off the site instead of letting it all infiltrate by containing optional underdrain systems in their gravel storage beds. They can be subjected to reduced hydraulic conductivity gradually due to clogging as well (Rossman, 2010).

LID controls within a subwatershed in SWMM can be placed two different ways:

1. One or more LID controls can be placed in an existing subwatershed that will displace an equal amount of non-LID area from the subwatershed;
2. create a new subwatershed devoted entirely to just a single LID practice.

The first approach is considered a mix of LIDs to be placed throughout a subwatershed, each treating a different portion of the runoff generated from the non-LID fraction of the subwatershed. Note that under this option the subcatchment's LIDs act in parallel. It is not possible to make them act in series (i.e., have the outflow from one LID control become the inflow to another LID) as shown in Figure 2.16.

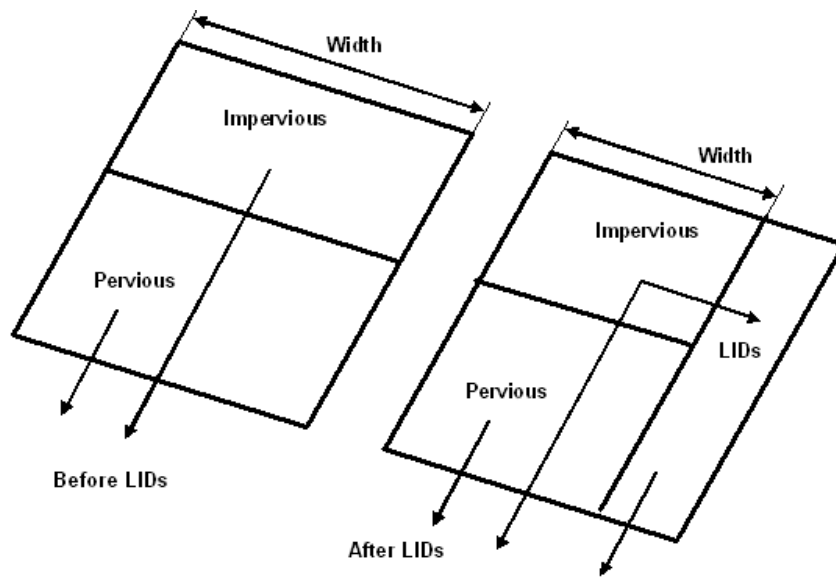


**Figure 2.16: Conceptualization of the surface runoff SWMM LID component**

## 2.5. Calibrated Strategy

Calibration was used for the modeling of TSBW. Manual calibration uses a subjective process of visual inspection and comparison of the model output and the observed data to evaluate implicitly (measure) the ability of the model to simulate specific aspects of the hydrologic behavior (Boyle et al., 2000). Subwatersheds draining to each site were first identified. The calibration process was then carried out from upstream to downstream direction. For instance;

Subwatersheds 1, 2, 5, 6, 7, 9, and 10, which drain into site 5 were first calibrated. Site 4, which receives water from subwatersheds 22, 28, 29, 31, 33, 34, and 35 was calibrated similarly. Once a subwatershed is calibrated, its parameters were kept same when a calibration is performed for another site further downstream. Parameters of the model are listed in Table 2.7.

**Table 2.7: SWMM input parameters**

Parameters	Value Range	References
Slope ( $S$ )-%	$\pm 20$	From GIS
Width ( $W$ )-%	$\pm 20$	From GIS
Manning's $n$ for impervious area ( $Nimp$ )	0.010-0.025 for concrete	McCuen et al (2002)
Manning's $n$ for pervious area ( $Nper$ )	0.15-0.80 for grass/tree	McCuen et al (2002)
Manning's $n$ for conduit ( $n$ )	0.011-0.015 for concrete	ASCE (2000)
D_storage for impervious area ( $Dm$ )-cm	0.13-0.38	ASCE (2000)
D_storage for pervious area ( $Dp$ )-cm	0.25-1.02	ASCE (2000)
Suction head ( $\psi$ )-cm	1.27-76.20	Rawls et al. (1982)
Hydraulic conductivity ( $K$ )-cm/h	0.025-6.35	NRCS (1982)
Initial deficit ( $\theta$ )	0.05-0.70	NRCS (1982)

## 2.6. Design Storms

To estimate peak flows for different return period storms (1, 2, 5, 10, 50 and 100), the SWMM was run with the calibrated model. The minimum required storm duration for a design storm

must be equal to or greater than the time of concentration of the watershed. Time of concentration ( $T_c$ ) is the time required for the entire watershed to contribute to runoff at the outlet for hydraulic design; this is calculated as the time for runoff to flow from the most hydraulically remote point of the drainage area to the point under investigation. Technical Release 55 published by the NRCS in 1986 presents procedures to calculate  $T_c$  (Cronshey et al., 1985). It partitions waterway as sheet flow, shallow concentrated flow, open channel flow or some combination of these and gives the related equation for each type of flow. Using the Manning kinematic solution; the time of concentration for the first part is calculated as (NRCS, 1986)

$$T_t = 0.007 * (nL)^{0.8} / (P2)^{0.5} * s^{0.4}$$

where  $T_t$  = travel time(hr),  $n$  = Manning's roughness coefficient,  $L$  = flow length (ft),  $P2 = 2$  year, 24 hours rainfall (in) and  $s$  = slope of hydraulic grade line.

After a maximum of 300 feet, sheet flow usually becomes a shallow concentrated flow. In this part, the average velocity is determined using (average velocities for estimating travel time for shallow concentrated flow):

$$\text{Unpaved } u = 16.1345 (s)^{0.5}$$

$$\text{Paved } u = 20.3282 (s)^{0.5}$$

where  $u$  = average velocity (ft/s),  $s$  = slope of hydraulic grade line (watercourse slope, ft/ft). The travel time is then estimated using the following equation:

$$T_t = L / 3600u$$

where  $u$  = average velocity (ft/s).

Open channels are assumed to begin where surveyed cross section information is obtained on an aerial photograph or where blue lines appear on USGS quadrangle sheets. Manning's equation is used to estimate average flow velocity.

$$u = \frac{1.49}{n} * r^{\frac{2}{3}} * S^{\frac{1}{2}}$$

where  $r$  = hydraulic radius (ft). The estimated  $u$  is used in the previous equation to obtain the travel time. Time of concentration is the summation of  $T_t$  values for the various consecutive flow segments. Based on the estimated time of concentration, storm duration is selected.

## **2.7. Floodplain Maps**

In order to determine the flood risk based on the floodplain extent and the inundated region boundaries, the river floodplain was simulated using the Hydrologic Engineering Center's River Analysis System (HEC-RAS). This software is used as a hydraulic routing model to analyze the river in both steady and unsteady states to obtain the floodplain boundaries, peak discharge and average depth for each cross section. Using HEC-GEORAS (US Army Corps of Engineers 2002), an ArcGIS extension specifically designed to process geospatial data for use with the HEC-RAS, the river cross sections were imported to the HEC-RAS and the streamflow predictions from Storm Water Management Model were transferred to the HEC-RAS model. The DEM resolution utilized in HEC-GEORAS was 3m by 3m, which was obtained from the USDA Natural Resources Conservation Service. In order to increase the accuracy of the cross sections, the cross sections surveyed during field trips were added to the cross sections obtained from the DEM. HEC-RAS was run in steady state using the peak flows obtained from SWMM for various return period storms; including 5, 10, 50, and 100-yr.

## 2.8. Flood Generating Areas

Kalin and Hantush (2009) developed an index-based, watershed model-driven approach that can assist in identifying sensitive areas in a watershed that could have larger or fewer impacts on low or high flows at a given specific location. The method is based on ranking different parts of a watershed based on their relative impacts on watershed responses such as peak flow and flooding to anticipate land developments. A similar approach was followed in this study. Two types of indices were used to explore the flood generating areas in this study. For this, each subwatershed was first disconnected from the watershed to determine their relative contributions to the peak flow (see also Saghafian and Khosroshahi 2005). Figure 2.17 shows how the proposed method is performed. This way one can identify the subwatersheds that have the highest contribution to downstream flow, and management efforts (such as LID practices) can concentrate on those areas. The first index does not take into account the size of the subwatersheds.

$$\alpha_j = (Q - Q_j)/Q$$

where  $Q$  is flow observed at the outlet when all subwatersheds contribute and  $Q_j$  is flow when all the subwatersheds except subwatershed  $j$  contribute to flow.

The second index compensates for the area of each subwatershed.

$$\beta_j = \alpha_j / (\frac{A_j}{A})$$

where  $A$ : Watershed area and  $A_j$ : Subwatershed ( $j$ ) area.

Both might be useful under different situations. The first index can be used for instance if flows can be reduced at the outlet of a subwatershed, such as by using a detention pond. The second is more useful if multiple LIDs are needed that are spread over the subwatershed, such as many rain gardens, rain barrels, etc.

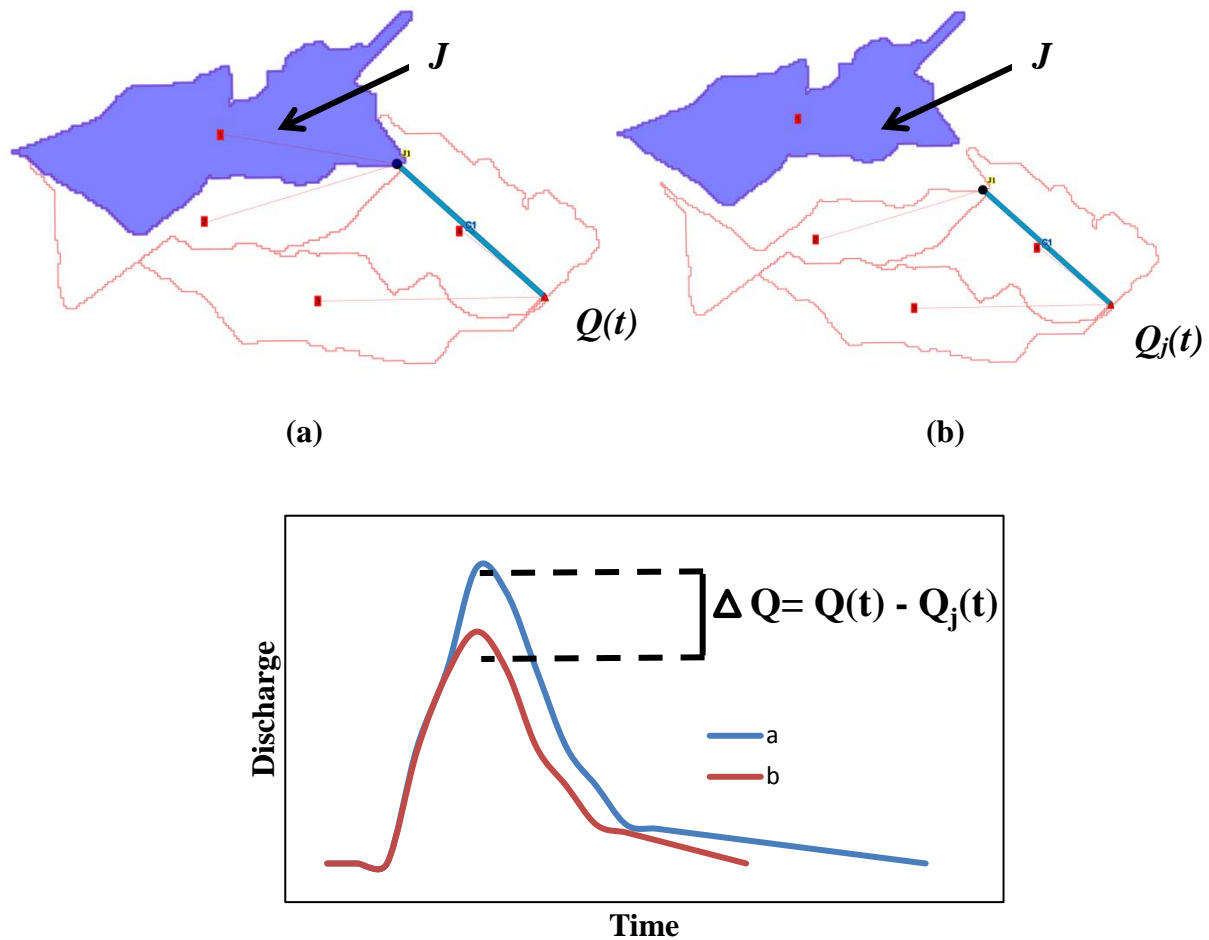


**Figure 2.17: Schematic representation showing the calculations of flood generating areas indices**

### 3. RESULTS

#### 3.1. Observed Stage Levels

Figure 3.1 and 3.2 shows the time series of measured stage levels at the five sites. Red lines show the bankfull stages. Bankfull stage was exceeded only ones at site 1 and 3, in spite of the extreme wet conditions (2015 was +15 inches above normal precipitation). One of the biggest rain events happened on September 9<sup>th</sup> 2015 and lasted 4 hours. The rain gauge measured 3.94 inches of precipitation. Radar-based rainfall estimate was 4.93. Figure 3.1 illustrates that the water level at site 1 was recorded at 2.99 *m* by the pressure transducer which is slightly higher than the maximum channel depth (2.91 *m*). In addition to site 1, water level at site 3 reached 1.85 *m* which is 22 *cm* higher than the bankfull level (1.63 *m*) as shown in Figure 3.1. The water level at the other sites was lower than the channel maximum depth (Figure 3.1 and 3.2). Observed maximum depth for each site during the period 9/19/2014 to 11/10/2015 is given in Table 3.1.

**Table 3.1: Observed maximum depth at each site during the period 9/19/2014 - 11/10/2015**

Site	Depth ( <i>m</i> )	Date
1	2.99	9/27/2015
2	3.22	9/27/2015
3	1.85	9/27/2015
4	1.49	9/27/2015
5	1.45	9/27/2015

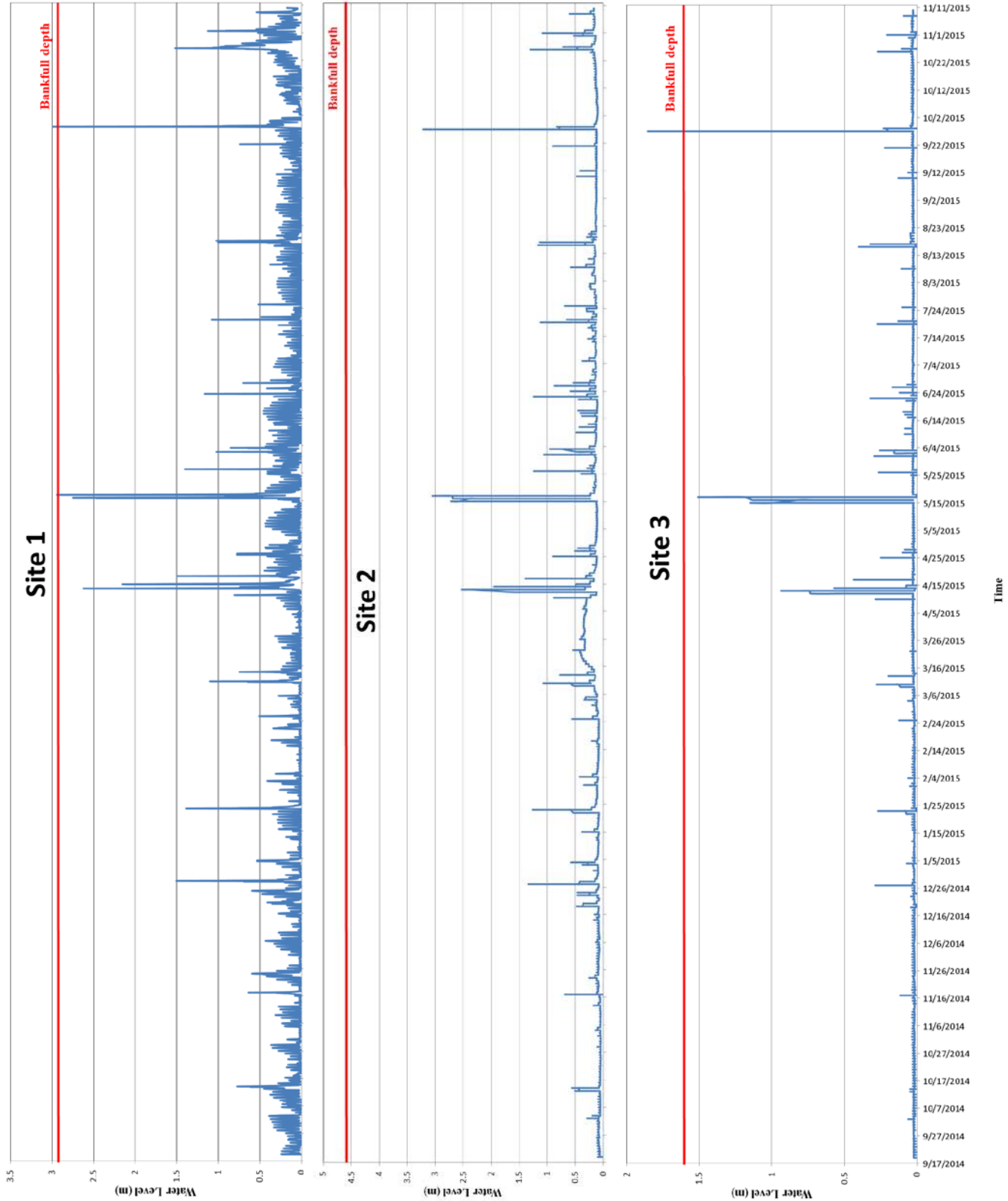


**Figure 3.1: Observed water depth at site 1 (top), site 2 (middle), and site 3 (bottom) from 9/19/2014 to 11/10/2015**

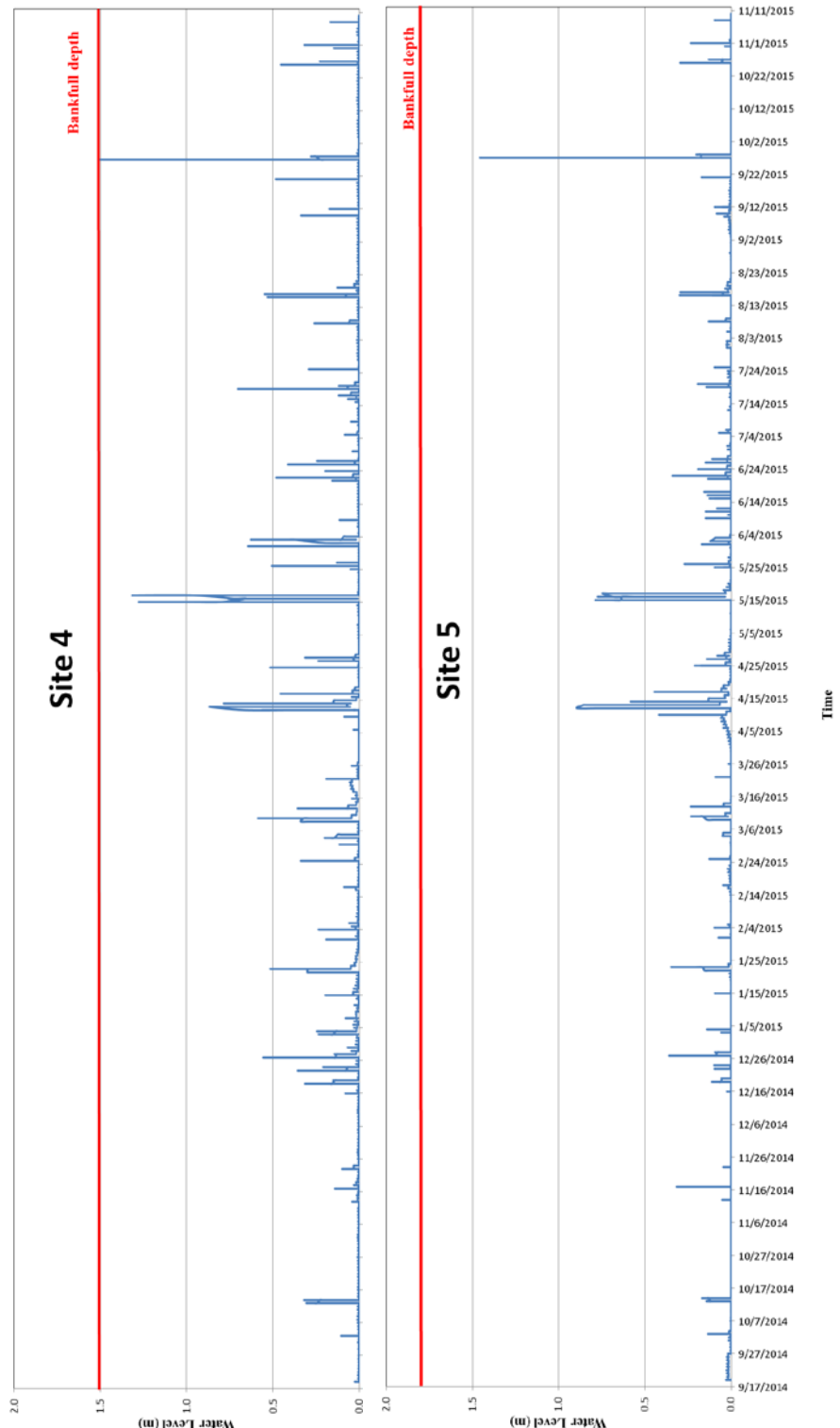


**Figure 3.2: Observed water depth at site 4 (top) and site 5 (bottom) from 9/19/2014 to 11/10/2015**

The observed data shows that there is no widespread flooding issue, at least along the TSB and its tributaries. Flooding reported by residents must be highly local and caused by secondary reasons. For instance; clogged channels and ditches were noticed during the field visits. These probably caused the water to back up and flood some local roads and the backyards of houses (Figure 2.6). In one case, after the city cleaned the debris from channel, one resident said that the water level significantly decreased and he did not see water back up problem anymore.

### **3.2. Model Performance**

The SWMM model was calibrated for water levels using data obtained at the 5 sites (Figure 2.8). Although some discharge measurements were taken during the field visits, the discharge data was not enough to calibrate the model for flow since most significant rain events happened at midnight or the peaks were missed. TSBW is a flashy watershed due to channelization. Therefore, the model was calibrated for water levels only using data obtained from those 5 sites. The water level (stage) estimates by the SWMM model were compared to stage data collected by the pressure transducers during the period 9/19/2014 to 11/10/2015. The most downstream site 1 is significantly influenced by tidal effect, which was treated as a lower boundary condition in the SWMM. In general, the model simulated water levels with an acceptable level of accuracy compared to the observed data; however, model overestimated water levels at site 5, which is the most upstream site (Figure 2.8). Figure 3.3 shows the simulated and observed water depth time series and the depth duration curves at site 5. The depth duration curves were limited to the top 5%, because this is a flooding study. Both simulated and observed rising limbs and the maximum flow depths timing are similar, but simulated falling limb lasts shorter than observed one. Overall, the shape of the simulated hydrograph matches the observed one well, including

maximum flow depths and volume (area under the depth hydrograph in this study). Figure 3.4 shows the simulated and observed water depth time series and the depth duration curve at site 4. Again the simulated rising limbs and time to the peaks are very similar, but simulated volume is a little under-predicted, and observed falling limb lasts a little longer. Figure 3.5 demonstrates simulated and observed water depth time series and the depth duration curve for site 3. The rising limb is again very much alike the simulated water depth, as well as time to the maximum flow depth, but volume and falling limb duration was under-predicted. Figure 3.6 represents simulated and observed water depth time series and the depth duration curve for site 2. The simulated volume was under-predicted, and the observed falling limb is longer. However, overall shape, maximum flow depth and rising limb match quite well. Figure 3.7 compares simulated and observed water depth time series and the depth duration curve from site 1 which is the most downstream site and is significantly influenced by the tidal effect. The volume and falling limb were under-predicted. However, shape, rising limb, and time to the peaks compare well. Overall, in most cases, the simulated water depth matches the observed water depth, but the model underestimated in very large water depths.

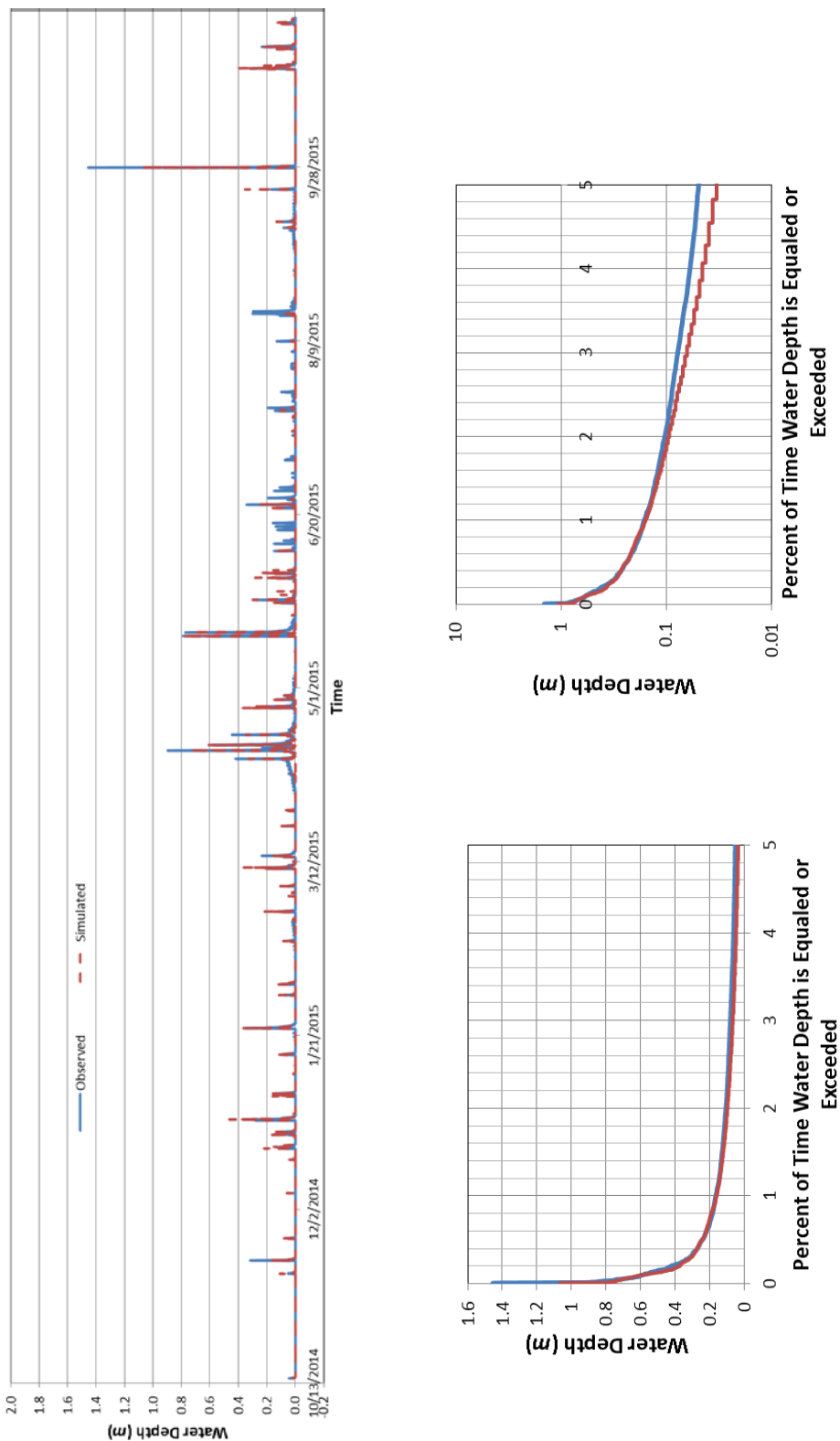


**Figure 3.3: Simulated/Observed water depth and Depth Duration Curve at site 5**

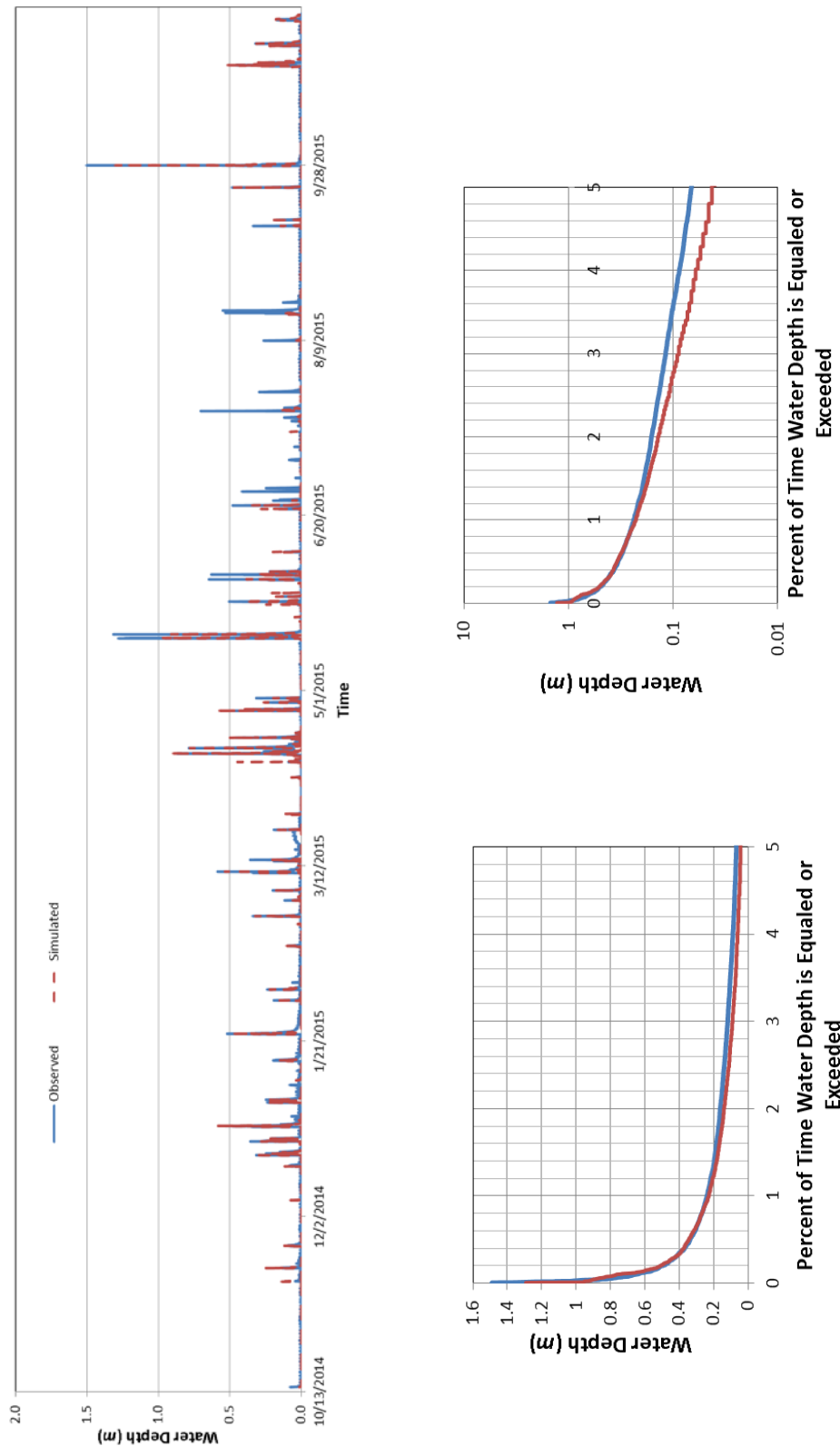


**Figure 3.4: Simulated/Observed water depth and Depth Duration Curve at site 4**

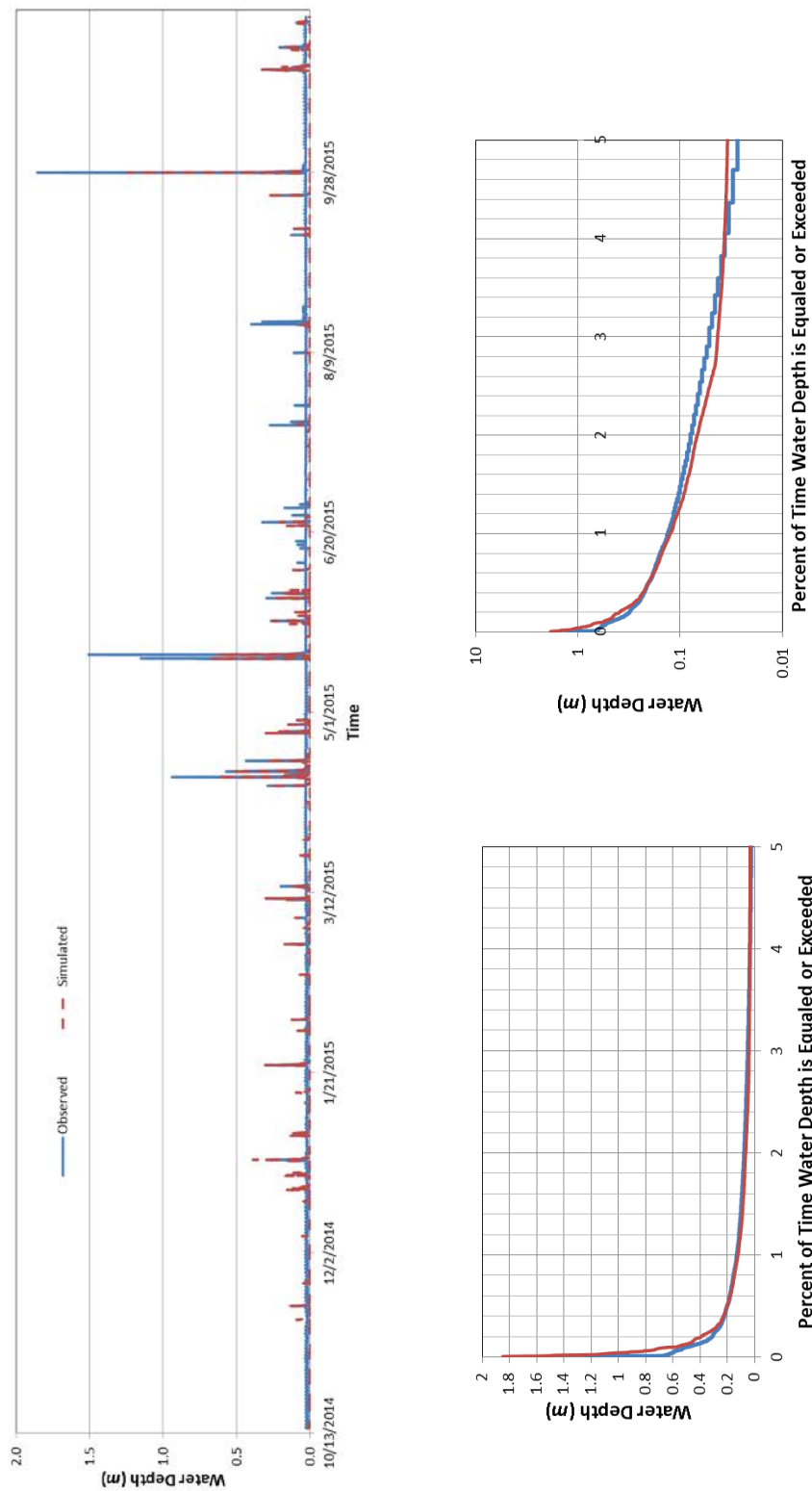


**Figure 3.5: Simulated/Observed water depth and Depth Duration Curve at site 3**

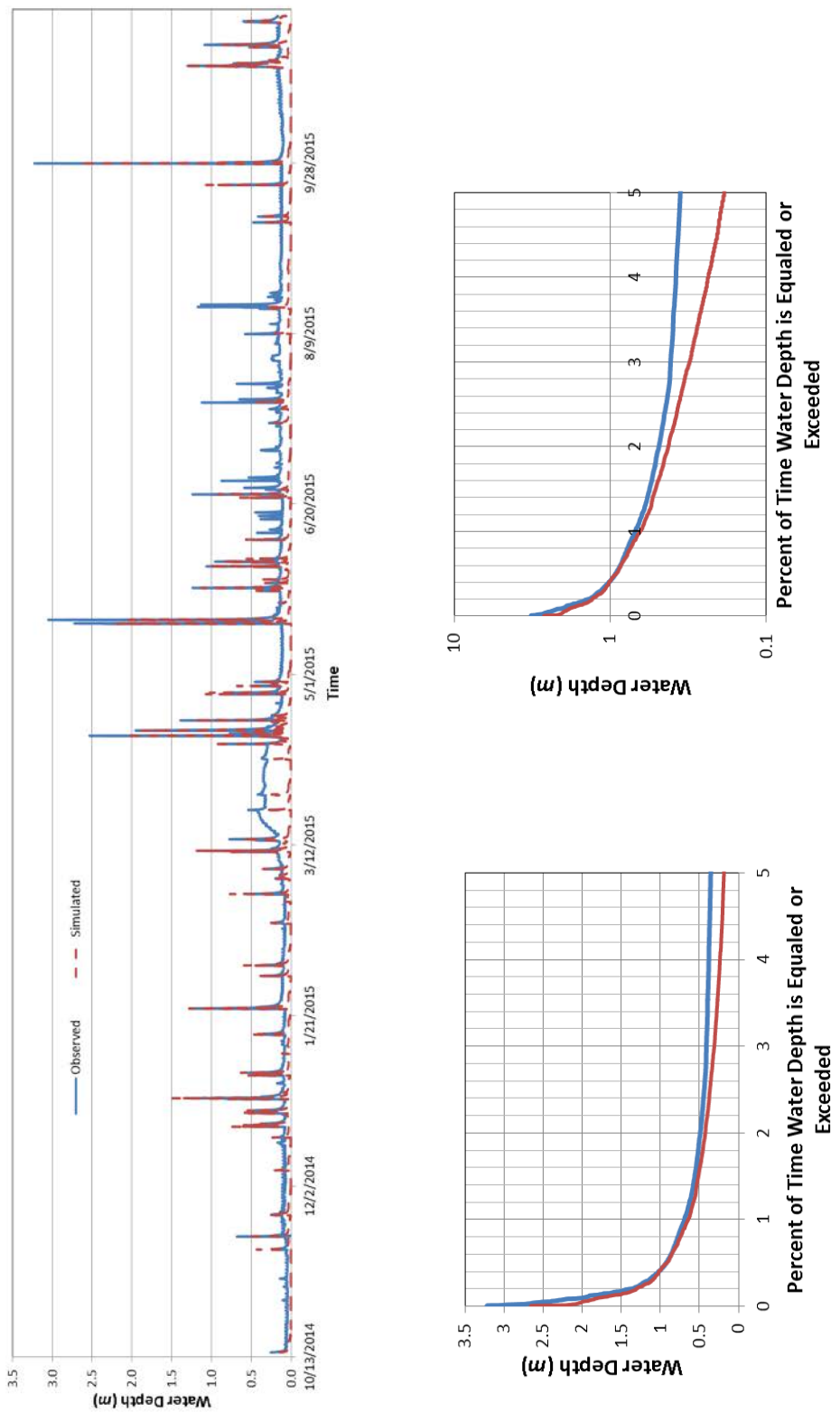


**Figure 3.6: Simulated/Observed water depth and Depth Duration Curve at site 2**

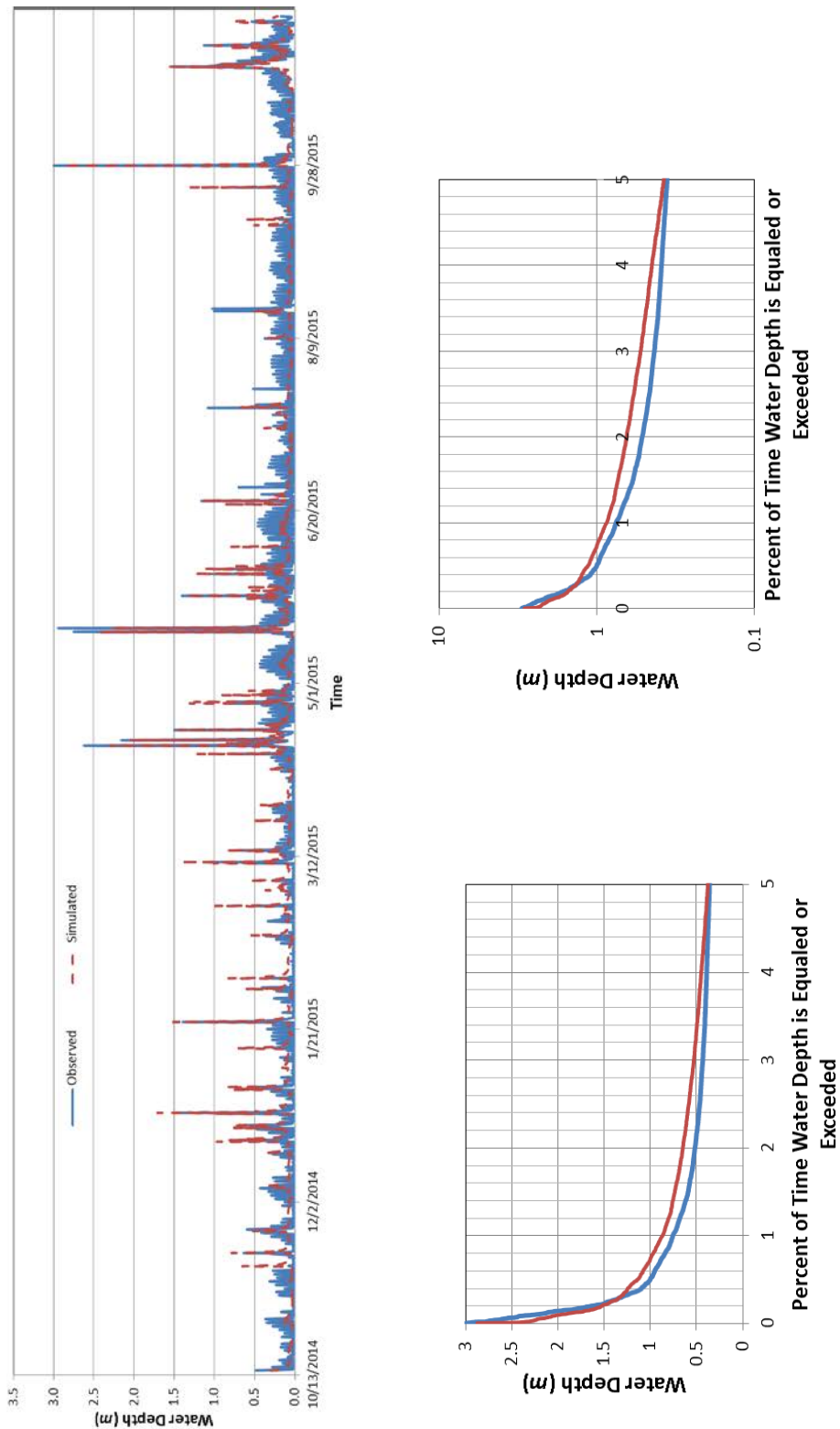


**Figure 3.7: Simulated/Observed water depth and Depth Duration Curve at site 1. Oscillations are tide effect**

Calibration parameters were obtained from the same studies of SWMM model (Liong et al., 1991; Choi and Ball, 2002; Fang and Ball, 2007; Rivas and Roesner, 2009). Table 3.2 shows the calibrated SWMM parameters. Hydraulic conductivity ( $K$ ) was found the most sensitive parameter.

**Table 3.2: The calibrated SWMM parameters**

<b>Subwatersheds</b>	<b><math>S</math> (%)</b>	<b><math>W</math> (%)</b>	<b><math>Nimp</math></b>	<b><math>Nper</math></b>	<b><math>n</math></b>	<b><math>Dm(cm)</math></b>	<b><math>Dp(cm)</math></b>	<b><math>\Psi(cm)</math></b>	<b><math>K</math> (cm/hr)</b>
1, 2, 5, 6, 7, 9, 10	+15	+10	0.01	0.15		0.38	0.25	10.99	0.254
3,4,8,11,12,13,14,15,16,1 7,18,19,20,21,22,23,24,25 ,26,27,28,29,30,31,32,33, 34,35,36	-15	-10				0.38	0.25	10.99	0.254
<b>Conduits</b>									
16 & 17					0.013				
9,10,11,12					0.040				
1,2,3,4,5,6,7,8,13,14,15,1 8,19,20,21,22					0.011				

The performance of the model was also assessed by plotting simulated versus observed maximum water depth values from each big event for all sites (Figure 3.8, 3.9, 3.10, 3.11, and 3.12). In addition to rain gauge, precipitation data from radar was also performed in the figures. In order to do this, hourly radar rainfall was disaggregated into 15 minute interval. As can be seen from the figures, both rain gauge and radar gives a good result for low depth events. In large depth events, radar gives a better result. Table 3.3 shows the values of coefficient of determination  $R^2$ , Nash-Sutcliffe efficiency ( $NSE$ ), and Percent bias ( $PBIAS$ ) for the calibration

events for each site.  $R^2$  describes the degree of collinearity between simulated and measured data.

$$R^2 = \left[ \frac{\sum_{t=1}^n (x_t^{obs} - x_{mean}^{obs})(x_t^{sim} - x_{mean}^{sim})}{\sqrt{\sum_{t=1}^n (x_t^{obs} - x_{mean}^{obs})^2 (x_t^{sim} - x_{mean}^{sim})^2}} \right]^2$$

$NSE$  is a normalized statistic that determines the relative magnitude of the residual variance compared to the measured data variance (Nash and Sutcliffe, 1970).

$$NSE = 1 - \left[ \frac{\sum_{t=1}^n (x_t^{obs} - x_t^{sim})^2}{\sum_{t=1}^n (x_t^{obs} - x_{mean}^{obs})^2} \right]$$

where  $x_t^{obs}$  is the  $t^{\text{th}}$  observation for the constituent being evaluated,  $x_t^{sim}$  is the  $t^{\text{th}}$  simulated value for the constituent being evaluated,  $x_{mean}^{obs}$  is the mean of observed data,  $x_{mean}^{sim}$  for the constituent being evaluated, and  $n$  is the total number of observations.

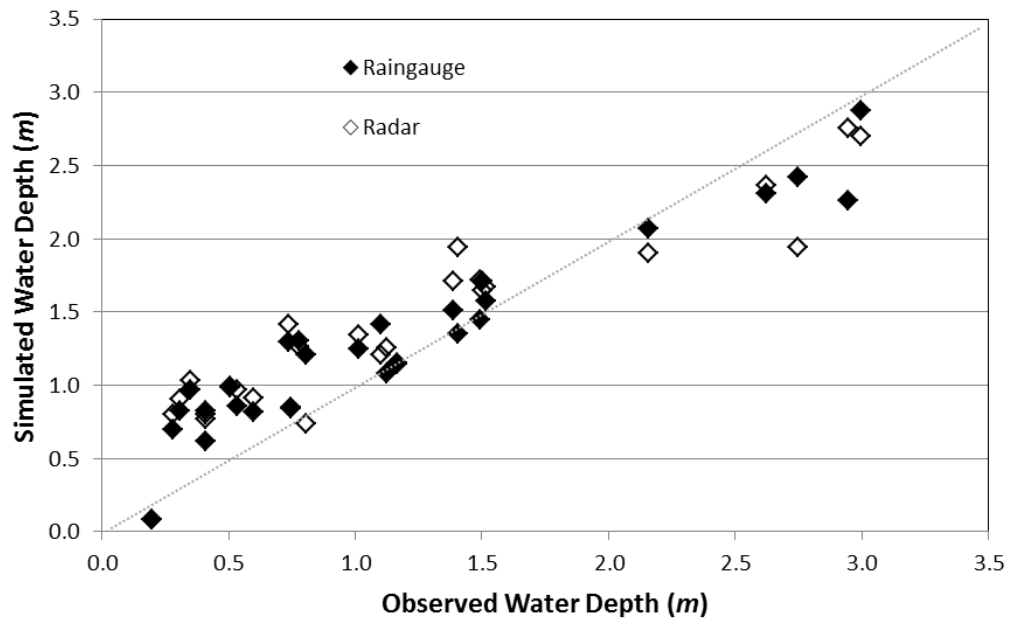
$PBIAS$  measures the average tendency of the simulated data to be larger or smaller than their observed counterparts (Gupta et al., 1999).

$$PBIAS = \left[ \frac{\sum_{t=1}^n (x_t^{obs} - x_t^{sim}) * (100)}{\sum_{t=1}^n (x_t^{obs})} \right]$$

where  $PBIAS$  is the deviation of data being evaluated, expressed as a percentage

**Table 3.3: Model performance statistics**

Sites	R <sup>2</sup>			NSE			PBIAS (%)		
	Rain Gauge	Radar	Best	Rain Gauge	Radar	Best	Rain Gauge	Radar	Best
1	0.91	0.86	0.93	0.83	0.78	0.88	-12	-16	-11
2	0.93	0.87	0.96	0.87	0.83	0.92	6	2	4
3	0.88	0.85	0.97	0.70	0.69	0.82	17	13	11
4	0.86	0.82	0.95	0.82	0.79	0.92	9	6	6
5	0.90	0.76	0.93	0.86	0.73	0.88	5	8	4

**Figure 3.8: Observed and simulated maximum depths during large storms using rainfall data from both raingauge and radar at site 1**

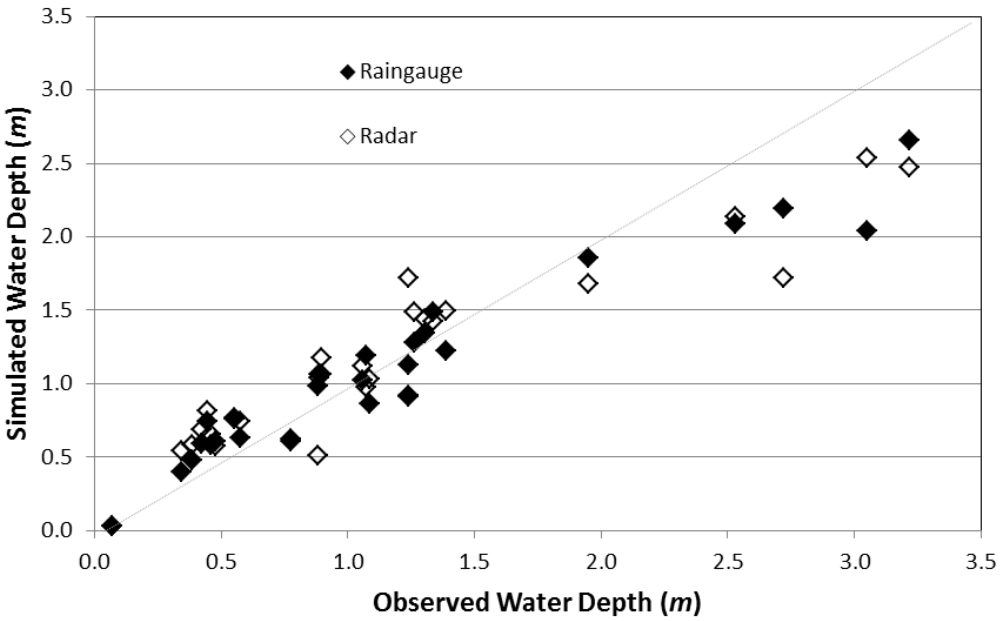


**Figure 3.9: Observed and simulated maximum depths during large storms using rainfall data from both raingauge and radar at site 2**

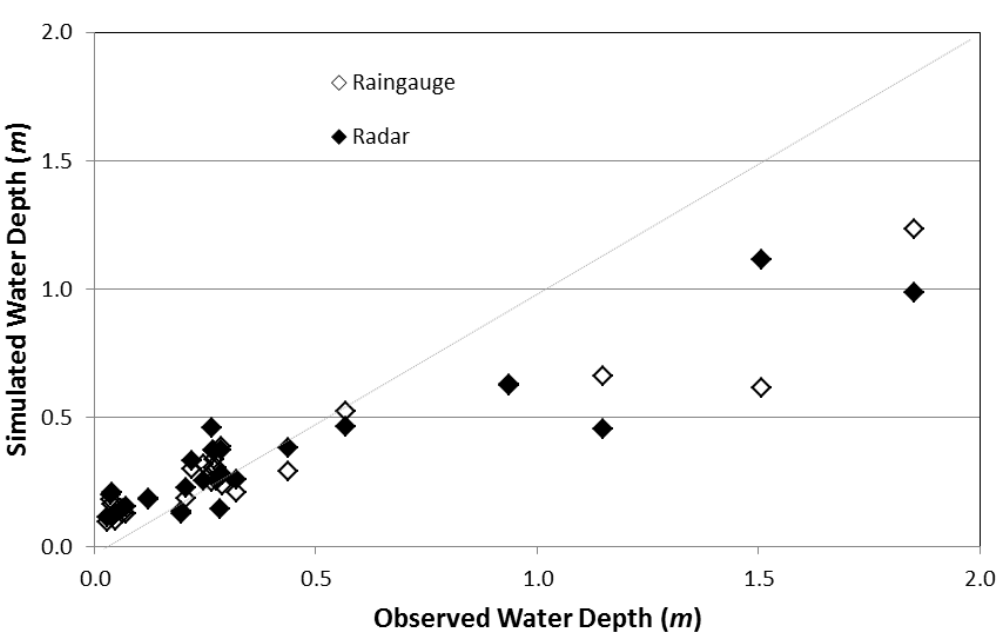


**Figure 3.10: Observed and simulated maximum depths during large storms using rainfall data from both raingauge and radar at site 3**

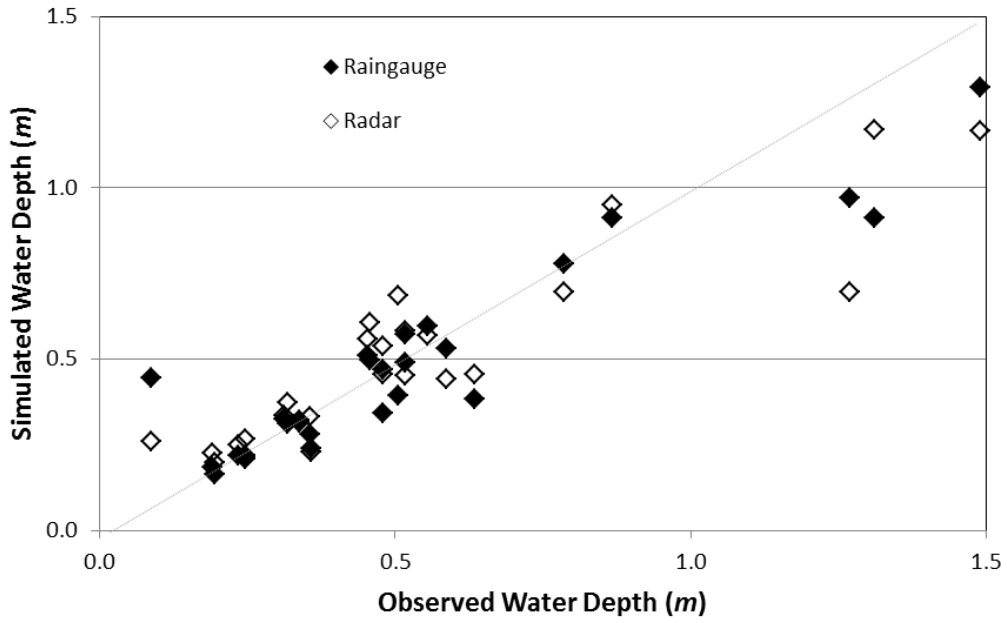


**Figure 3.11: Observed and simulated maximum depths during large storms using rainfall data from both raingauge and radar at site 4**

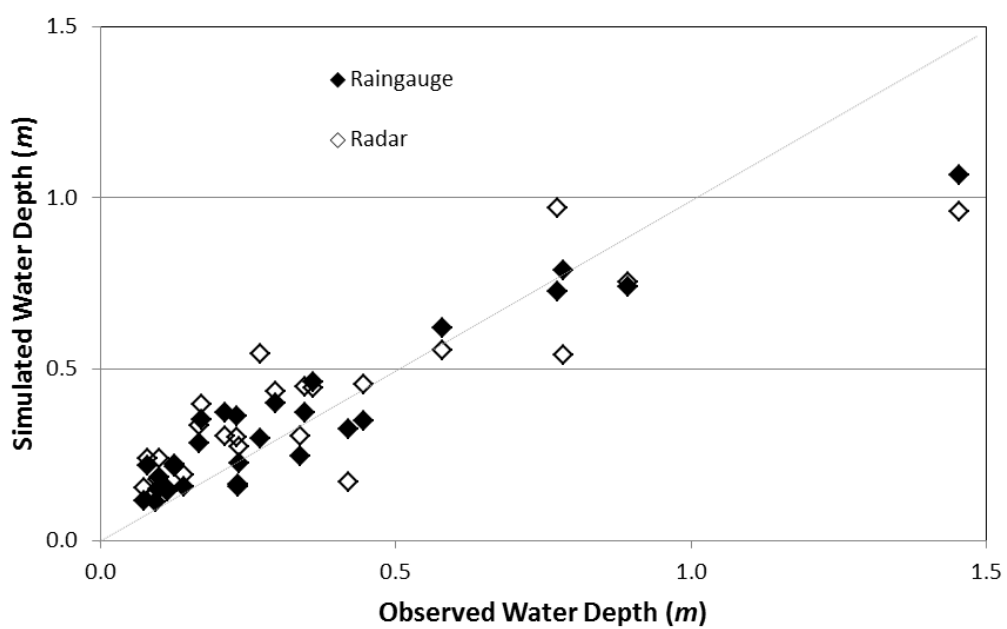


**Figure 3.12: Observed and simulated maximum depths during large storms using rainfall data from both raingauge and radar at site 5**

### 3.3. Design Storms

Based on the estimated time of concentration (Table 3.4), 2 hour storm duration was selected. Storm intensity was obtained from the National Oceonic and Atmospheric Administration website: <http://hdsc.nws.noaa.gov/hdsc/pfds/>.

**Table 3.4: Estimation of time of concentration**

Flow Segments	Tc (hr)
Sheet flow	0.39
Shallow concentrated flow	1.02
Open channel flow	0.42
$Tc=Tt1+Tt2+Tt3$	1.83

In order to obtain the rainfall hyetograph or distribution, the rainfall distribution type was determined using the geographic representation of NRCS storm types. The study area is located in type III as shown in Figure 3.13. NRCS provides cumulative distribution for one inch rainfall over a 24-hour period which can be used to generate design hyetograph for any duration and depth of rainfall. For this, the cumulative fraction was first scaled to 2-hr duration design storm depth. Then by multiplying the design storm depth with the fractions, the cumulative rainfall values were obtained. The incremental rainfall depths were then calculated by subtracting consecutive values. Table 3.5 rainfall depths for 2-hr duration storms of varying return period. Also, Figure 3.14 shows 2 hour rainfall hyetograph for a 5-year return period storm.

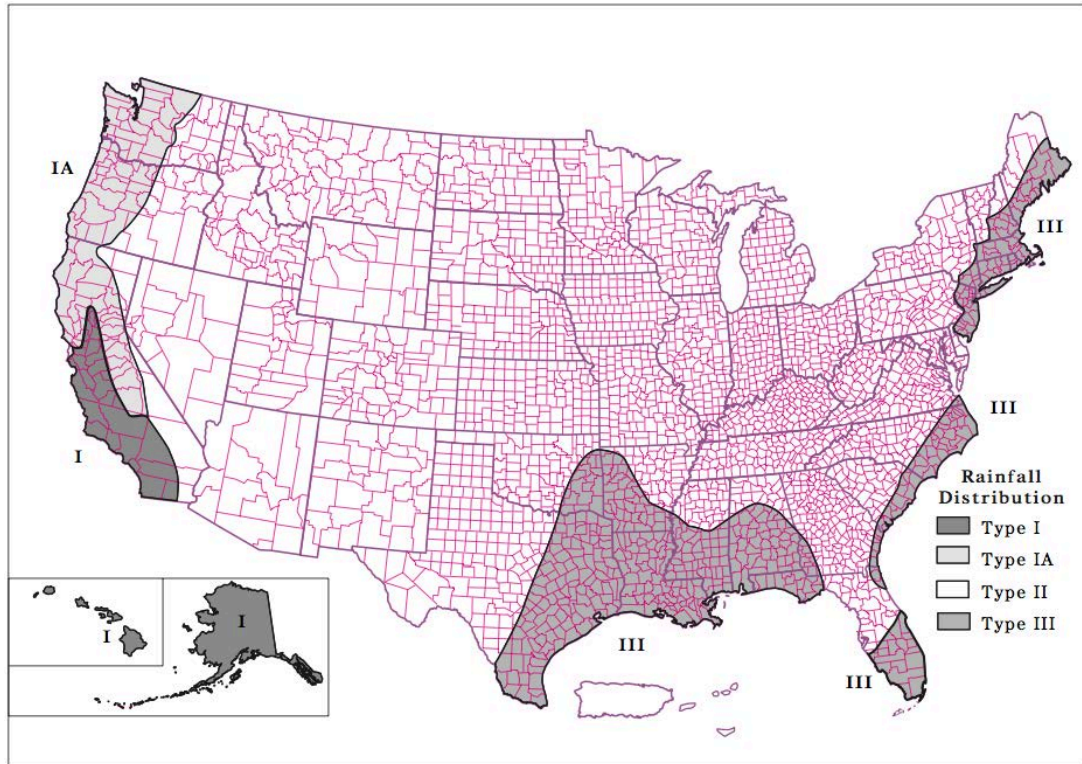


**Figure 3.13: Approximate geographic boundaries for NRCS (SCS) rainfall**

**Table 3.5: 2 hour duration storm depths for different return periods**

Return period	Rainfall (inch)
1-yr	2.57
2-yr	2.94
5-yr	3.56
10-yr	4.1
25-yr	4.89
50-yr	5.54
100-yr	6.92

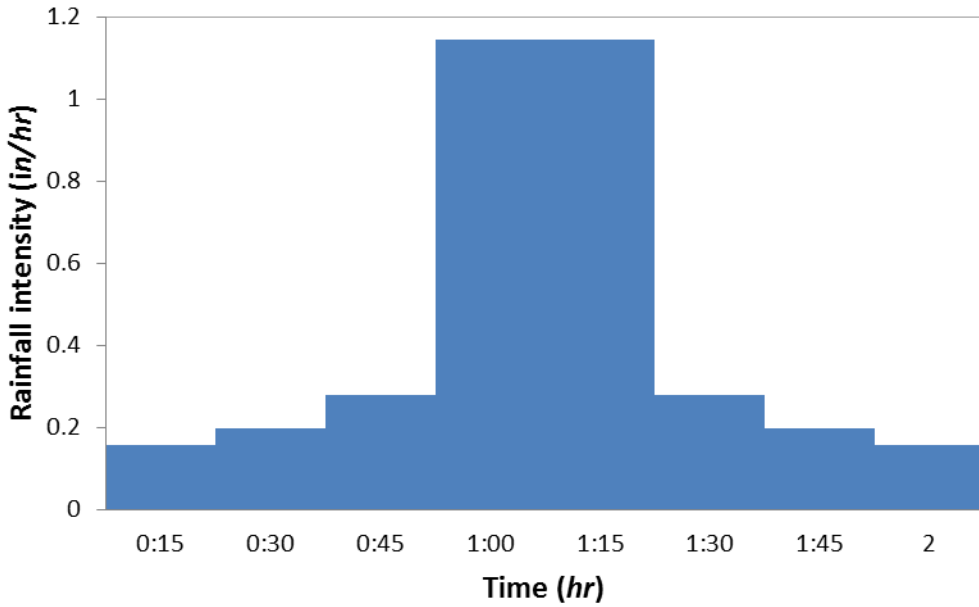


**Figure 3. 14: 2-hour rainfall hyetograph, 5-yr return period**

After estimating the design storm intensity and the rainfall hyetograph, the calibrated SWMM model was run to identify areas sensitive to flooding using design storms with 1, 2, 5, 10, 50, and 100 year return periods. Water depths at junctions (each subwatershed drains to an outlet, which are defined as *junctions* in the model) were assessed with each storm. Flooding is assumed to occur at junctions whenever the water depth exceeded the maximum depth. Note that inundation of junctions is function of the depth, intensity and duration of rainfall events. Results indicate that increasing storm depth and the return period led to increase in maximum water depth at junctions, number of junctions being inundated, flow volume, and duration of overflow (inundation). When the return period is 1 or 2 years, there is no overflow in any of the junctions, which means there is no urban flooding. Table 3.6 summarizes the duration of inundation of each junction under different return period storms, and Figure 3.15 shows the locations of the junctions that overflow for a 100 year storm.

**Table 3.6: Overflowing junctions and the duration of overflows for 5, 10, 50, and 100-yr return period storms. Design storm duration is 2 hours in each, which is roughly equal to the time of concentration of the TSB watershed**

<b>5 year – 3.56”</b>		<b>10 year – 4.1”</b>	
<b>Junction</b>	<b>Hours Flooded</b>	<b>Junction</b>	<b>Hours Flooded</b>
J28	0.35	J28	0.47
J11	0.30	J11	0.44
J16	0.23	J20	0.4
J20	0.21	J16	0.34
<b>100 year - 6.21”</b>		J26	0.30
		J13	0.21
<b>Junction</b>		<b>50 year - 5.54”</b>	
<b>Junction</b>	<b>Hours Flooded</b>	<b>Junction</b>	<b>Hours Flooded</b>
J20	1.12	J20	0.84
J11	0.98	J11	0.82
J28	0.82	J28	0.73
J26	0.81	J26	0.66
J16	0.76	J16	0.63
J13	0.69	J13	0.57
J2	0.46	J2	0.35
J6	0.38	J6	0.28
J3	0.34	J3	0.24
J19	0.31	J19	0.23
J10	0.09		

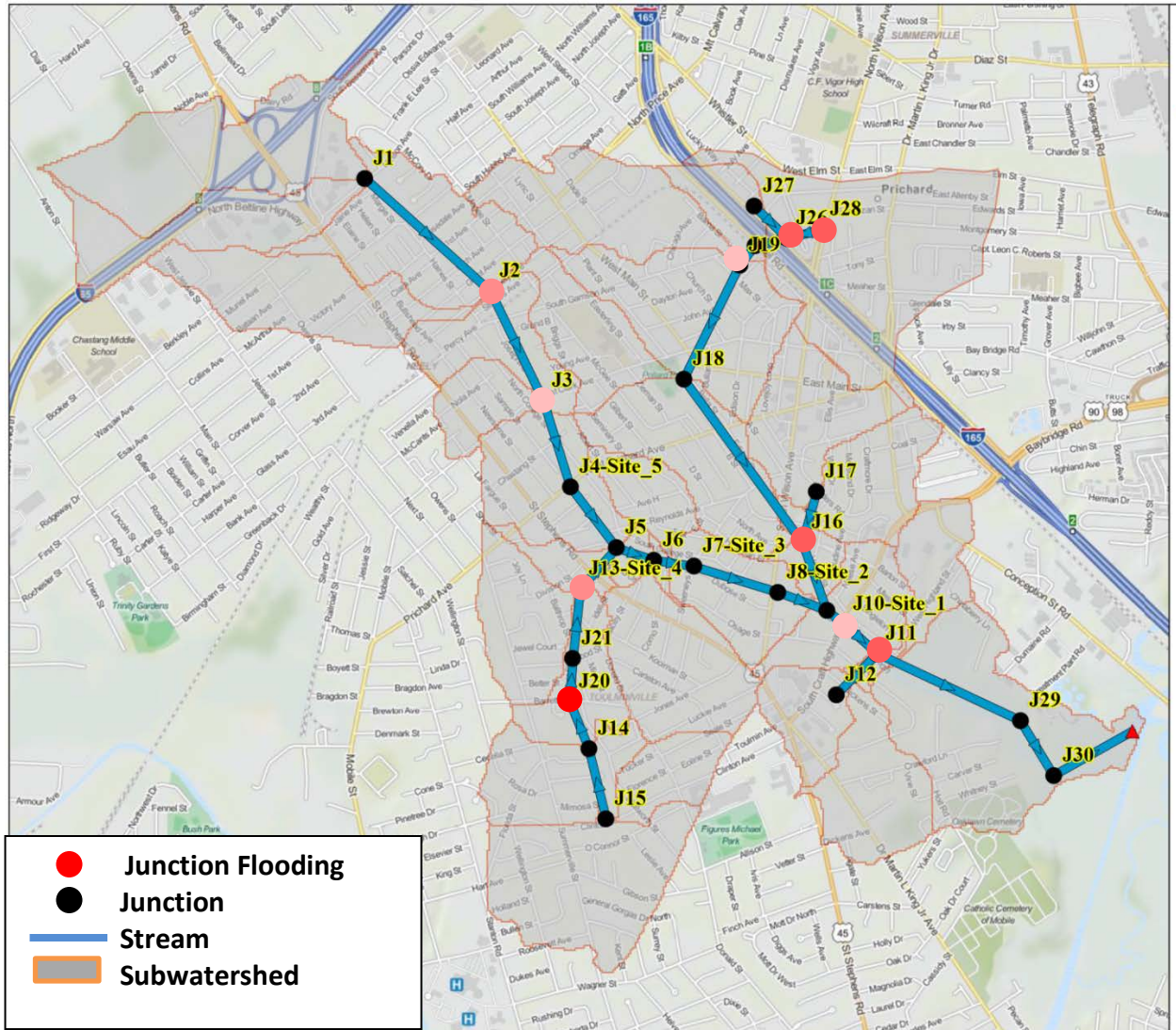


**Figure 3.15: Overflowing junctions under a 100-yr return period storm. The coloring scheme is representative of inundation duration. Junctions shown in black indicate no inundation at all, whereas dark red junctions are exposed to longer inundation periods compared**

Junctions 11, 16, 20, and 28 were the overflowing junctions for a 5 year return period event, which is more frequent than 10, 50, and 100 year events. J20 and J28 as overflowing junctions were studied further. Junction 11 was one of the most downstream junctions where there is very little urban development or residential area in the vicinity. Therefore, junction 11 was not

considered. Since junction 16 is outlet of 2 different closed conduits, it was not considered either. Note that J20 and J28 are among the most flood prone sites for all return periods (see Table 3.6). Both junctions are always in the top three flooded junctions.

### **3.4. Floodplain Maps**

Floodplain maps were generated for various return period storms including 5, 10, 50, and 100-yr. For this, streamflow predictions from the SWMM model were transferred to the HEC-RAS model. Areas susceptible to flooding were determined from these maps. Figure 3.16 shows the HEC-RAS generated 100-yr floodplain map as an example. Based on the extent of the floodplain map, there are four major flood prone areas. The southeast section on the map is mostly wetlands. Thus, there is no need of mitigation efforts here. The northwest part of the TSBW also appears highly flood prone. Interstate 65 is just upstream of this area with a large intersection, which has complex drainage network with underground drains. Therefore, this part of TSBW was not considered either for LID practices. The two junctions identified for further analysis earlier, i.e. J20 and J28, are located in the southwest and northeast flood prone sections shown in Figure 3.16, respectively. The 5, 10 and 50 year floodplain maps presented similar results. Therefore, flood generating area indices will be calculated for junctions 20 and 28 only. Although the analyses were limited to J20 and J28, similar analyses can be easily carried out for any other junctions.

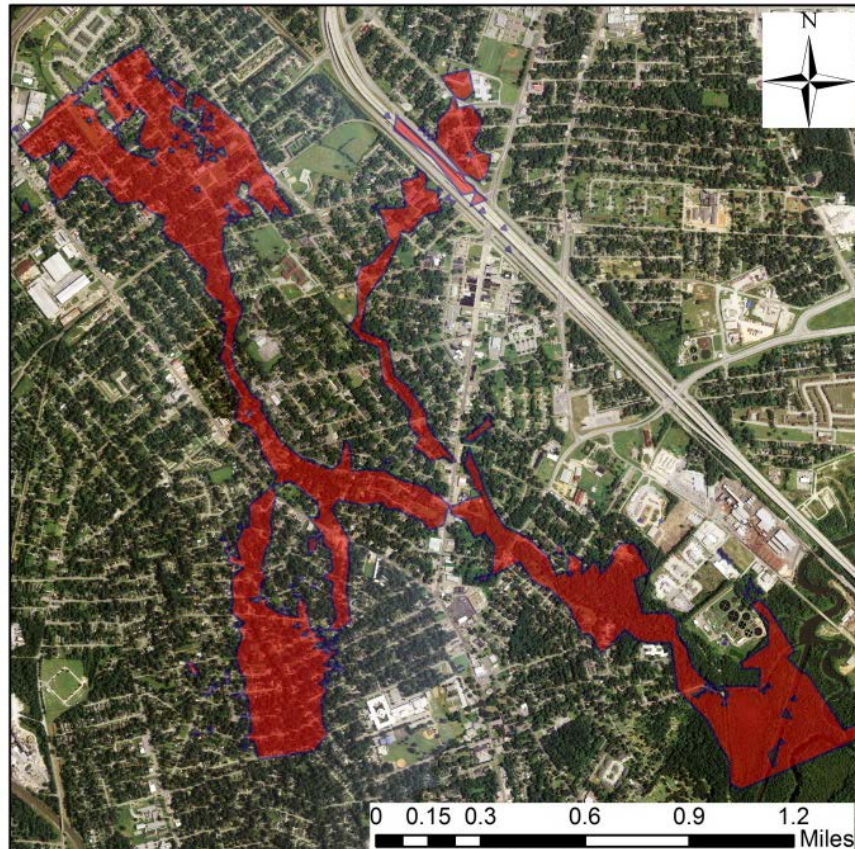


**Figure 3.16: 100- yr return period floodplain map shown on aerial photo**

### 3.5. Flood Generating Areas Index

The flood generating areas were studied under a 5 year storm, which is a more frequent event than a 100-yr storm. Based on 5 year storm, junction 20 and 28 were selected for further investigation. Two types of indices were used to explore the flood generating areas. Since there is only one subwatershed draining into junction 28, subwatershed 36 was selected for further study. Junction 20 receives water from subwatersheds 31, 33, 34, and 35. Based on the first index, subwatershed 35 was selected and subwatershed 34 was considered based on the second index for further study. The calculated indices for junction 20 are shown in Figure 3.17.

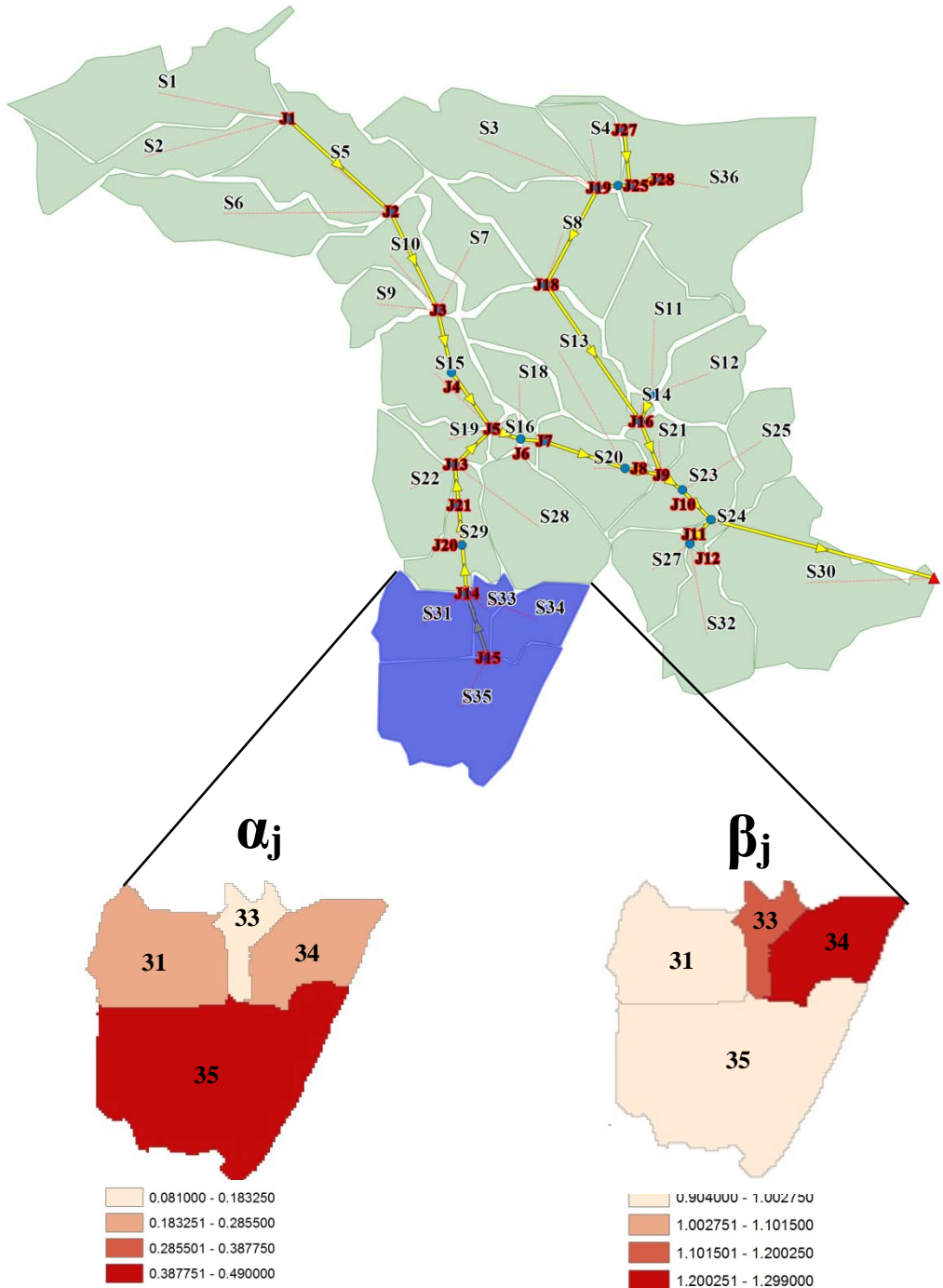


**Figure 3.17: Flood generating areas index at junction 20 and 28**

Based on flood generated area index for junction 20, subwatershed 34 has highest per unit area contributions to the peak flow at junction 20. However, if management efforts (LIDs) are

concentrated on subwatershed 34, the flooding at subwatershed 35 would not be considered since part of the subwatershed becomes inundated based on the 5-yr return period floodplain map (Figure 3.18) and the subwatershed was the flood generating area based on calculation of the first index. Therefore, mitigation efforts (Low impact development practices) were concentrated on the subcatchments 34, 35, and 36.

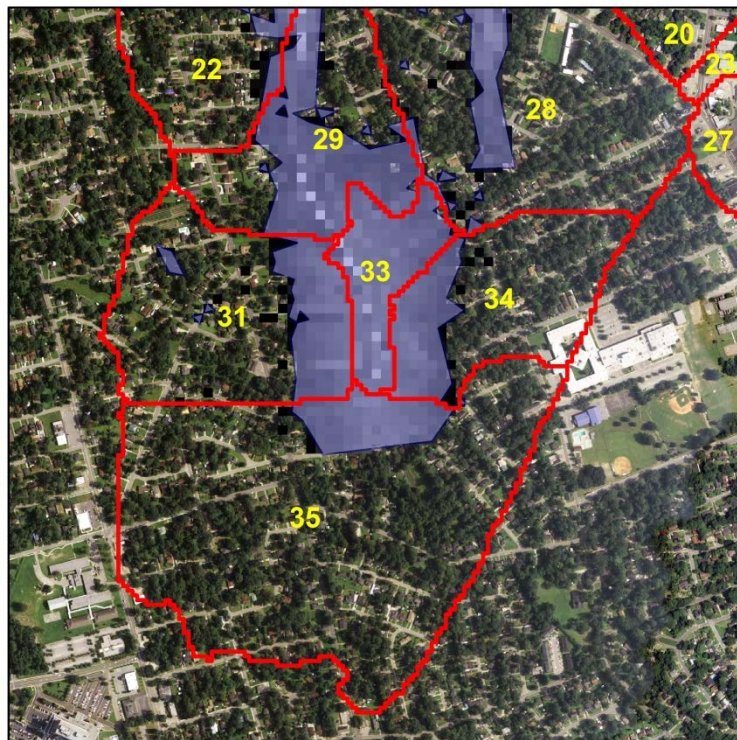


**Figure 3.18: Flooded areas 5-yr return period floodplain map**

## 3.6. SWMM LID Scenario

### 3.6.1. Rain Barrels and Cisterns

170 buildings were identified in subwatershed 34 occupying 19% of the total subwatershed area, 440 buildings in subwatershed 35 occupying 15.4% of the total subwatershed area, and 434 buildings in subwatershed 36, occupying 9.3% of its area using the city map of Prichard obtained from the city of Mobile's GIS department as shown in Figure 3.19. Once the buildings were identified, randomly 20 houses were picked within each subwatershed and the roof area of each building was calculated. Average roof area is 1,653 sq feet for subwatershed 34, 1,713 sq feet for subwatershed 35, and 1,662 sq feet for subwatershed 36. 200 gallon rain barrels were simulated for 85 houses and 1500 gallon cisterns were simulated for the rest of the buildings within subwatershed 34. 200 gallon rain barrels were simulated for 220 houses and 1500 gallon cisterns were simulated for the rest of the buildings within subwatershed 35. 200 gallon rain barrels were used for 217 houses and 1500 gallon cisterns were used for the rest of the buildings within subwatershed 36. Note that 200 gallon rain barrel does not necessarily mean a single rain barrel; it could be 2 to 4 smaller size rain barrels.

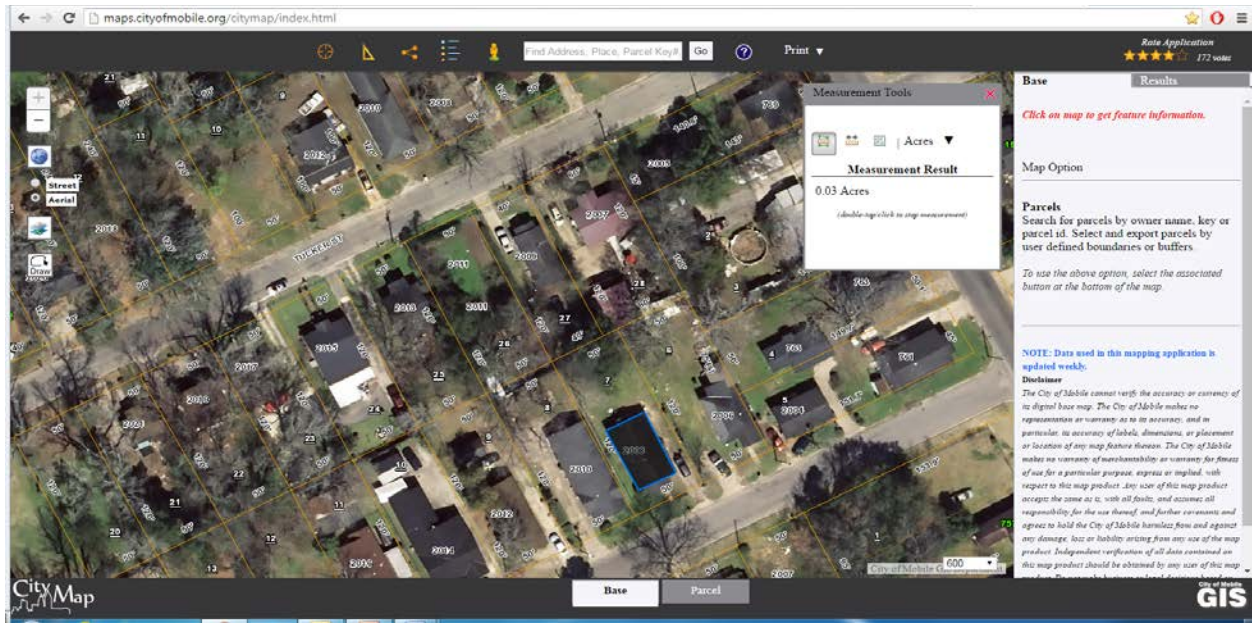


**Figure 3.19: Identifying and estimating the roof areas of the buildings using the city map of Prichard**

### 3.6.2. Permeable Pavements

Possible parking areas were identified and their areas were calculated using the city map of Prichard obtained from the city of Mobile's GIS department as shown in Figure 3.20. In subwatershed 35, parking lots occupy 0.9 % of the total subwatershed area. In subwatershed 36 they occupy 1.2% of the total subwatershed area. There is no potential parking lot area for the use of permeable pavements in subwatershed 34, therefore permeable pavements were not considered as LID options.

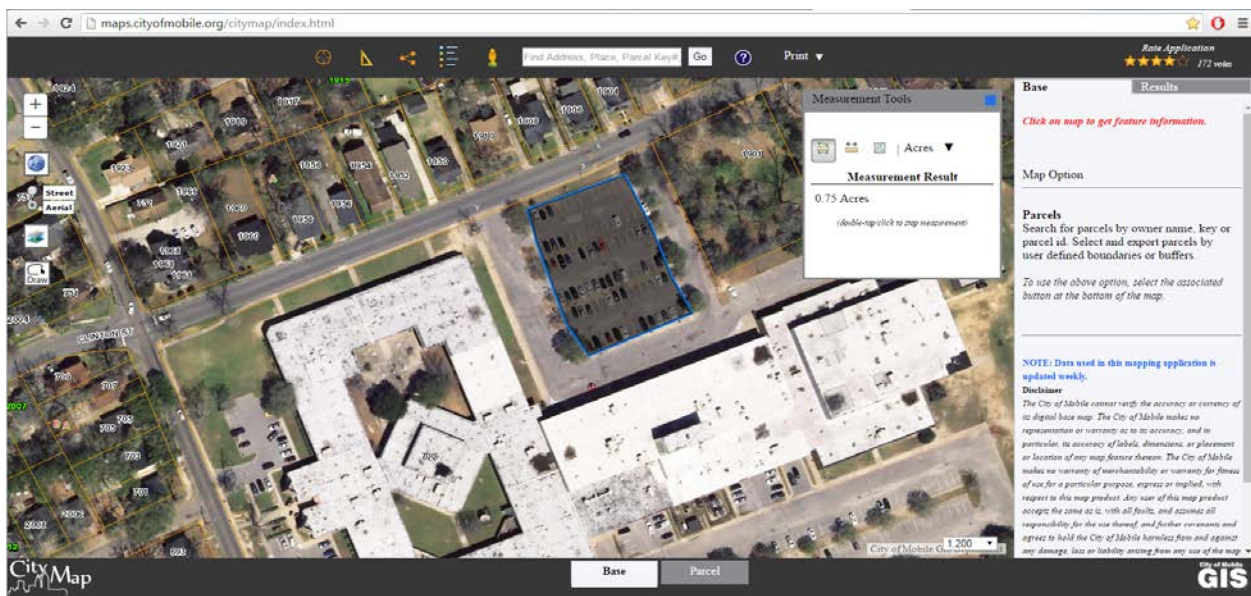


**Figure 3.20: Identifying and estimating the parking lot areas using the city map of Prichard**

Table 3.7 shows the reduction in peak flow, maximum depth and runoff volume at junction 20 based on subwatershed 34 under rain barrel as the only LID options. LID practices under different year return period can reduce peak flow by about 4-7%, depth by nearly 2-5% and runoff volume by approximately 1-3%.

**Table 3.7: Reduction in peak flow, depth, and runoff volume at junction 20 based on subwatershed 34 under the use of various LIDs and with different return periods**

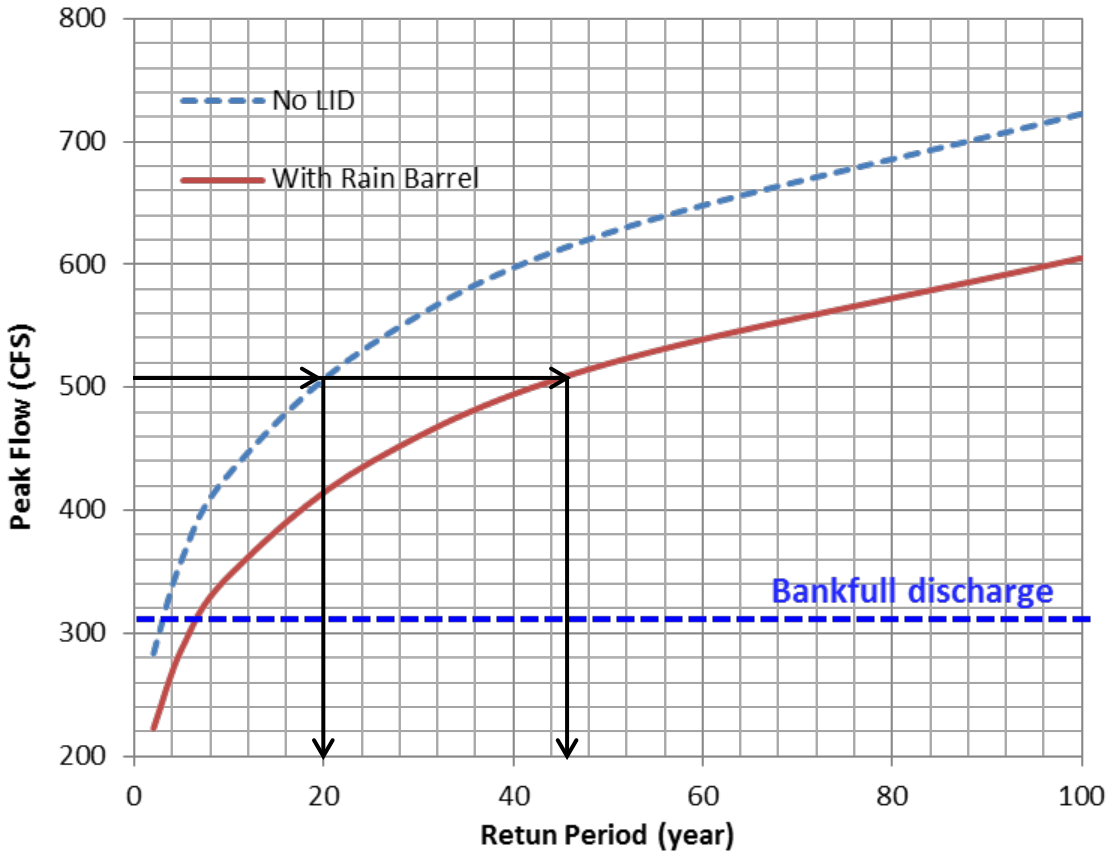
<b>Rain Barrel (RB)</b>	<b>Design Storm (year)</b>					
	<b>2</b>	<b>5</b>	<b>10</b>	<b>25</b>	<b>50</b>	<b>100</b>
Peak Flow Reduction (%)	7.3	6.8	6.2	5.1	4.6	4.4
Depth Reduction (%)	4.8	4.3	3.8	3.1	2.7	2.4
Runoff Reduction (%)	2.6	1.9	1.5	1.2	1.0	0.8

Table 3.8 shows the reduction in peak flow, runoff volume, and maximum water depth at junction 20 under various LID options which is just downstream of subwatershed 35, and within subwatershed 29. LID controls under different year return periods can decrease peak flow by approximately 18-24%, depth by about 5-15%, and runoff volume by nearly 4-10%. As can be seen from the tables, the effectiveness of LID practices are reduced with increasing return period.

**Table 3.8: Reduction in peak flow, depth, and runoff volume at junction 20 based on subwatershed 35 under the use of various LIDs and with different return periods**

<b>Rain Barrel (RB)</b>	<b>Design Storm (year)</b>					
	<b>2</b>	<b>5</b>	<b>10</b>	<b>25</b>	<b>50</b>	<b>100</b>
Peak Flow Reduction (%)	21.5	20.2	19.3	17.9	17.0	16.2
Depth Reduction (%)	14.3	12.8	11.7	10.6	8.4	4.8
Runoff Reduction (%)	8.6	6.3	5.0	3.8	3.1	2.6
<b>Permeable Pavement (PP)</b>						
	<b>2</b>	<b>5</b>	<b>10</b>	<b>25</b>	<b>50</b>	<b>100</b>
Peak Flow Reduction (%)	2.4	2.3	2.3	2.1	1.9	1.8
Depth Reduction (%)	1.6	1.6	1.2	1.1	0.9	0.9
Runoff Reduction (%)	1.9	1.7	1.6	1.5	1.4	1.4
<b>RB+PP</b>						
	<b>2</b>	<b>5</b>	<b>10</b>	<b>25</b>	<b>50</b>	<b>100</b>
Peak Flow Reduction (%)	23.3	22.0	21.0	19.6	18.7	17.9
Depth Reduction (%)	15.4	14.0	13.0	11.6	9.0	4.9
Runoff Reduction (%)	10.3	7.9	6.5	5.2	4.5	3.9

Figure 3.21 shows the peak flow rates under varying return period events with no LID and with rain barrel as the only LID. Because porous pavements have minimal impact (see Table 3.8), it was not considered here. The benefit of using rain barrels is clear from the figure. For instance, a 20 year maximum flow based on the current conditions (~510 cfs) can be expected to become a 46 year storm once the suggested rain barrels are installed. Similarly, as of now the bankfull stage flow (~313 cfs) is expected to happen on average every 3 years. The use of rain barrels as LID practices can convert this into a 6 year event.



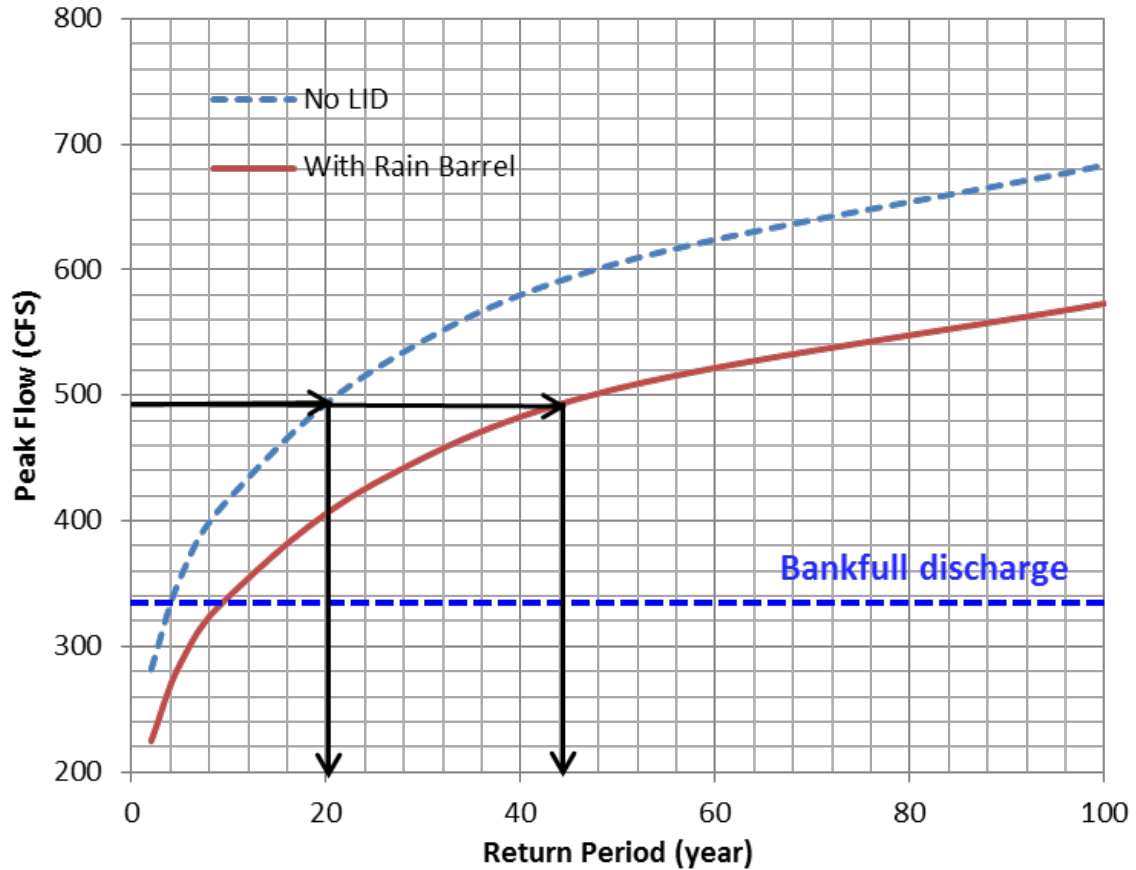
**Figure 3.21: Variation in peak flows under various return periods with and without LID (only rain barrel was considered) implemented at junction 20 based on subwatershed 35**

Table 3.9 shows the reduction in peak flow, depth, and volume under various LID options at junction 28, which receives all the runoff from subwatershed 36. Based on the table, LID controls under different year return periods can decrease peak flow by approximately 20-25%, depth by 11-16%, and runoff volume by nearly 14-24%. As can be seen from the table, the effectiveness of LID controls are again reduced with increasing return period.

**Table 3.9: Reduction in peak flow, depth, and runoff volume at junction 28 based on subwatershed 36 under the use of various LIDs and with different return periods**

<b>Rain Barrel (RB)</b>	<b>Design Storm (year)</b>					
	<b>2</b>	<b>5</b>	<b>10</b>	<b>25</b>	<b>50</b>	<b>100</b>
Peak Flow Reduction (%)	20.2	19.2	18.6	17.4	16.5	16.1
Depth Reduction (%)	11.7	10.9	10.5	9.5	8.8	8.7
Runoff Reduction (%)	18.7	16.3	14.8	11.7	10.0	9.6
<b>Permeable Pavement (PP)</b>						
Peak Flow Reduction (%)	<b>2</b>	<b>5</b>	<b>10</b>	<b>25</b>	<b>50</b>	<b>100</b>
	4.9	4.9	4.9	4.8	4.7	4.7
	2.8	2.8	2.6	2.4	2.3	2.3
Depth Reduction (%)	5.3	5.1	5.0	4.7	4.5	4.5
	<b>2</b>	<b>5</b>	<b>10</b>	<b>25</b>	<b>50</b>	<b>100</b>
	24.6	23.6	22.9	21.7	20.8	20.4
RB+PP	14.5	13.6	13.0	12.0	11.4	11.1
	23.5	21.0	19.4	16.1	14.2	13.9

Figure 3.22 shows the peak flow rates under varying return period events with no LID and with rain barrel as the only LID. Because porous pavements have minimal impact, it was not considered on the figure. The benefit of using rain barrels is clear from the figure. For instance, a 20 year maximum flow based on the current conditions (~495 cfs) can be expected to become a 44 year storm once the suggested rain barrels are installed. Similarly, as of now the bankfull stage flow (~333 cfs) is expected to happen on average every 4 years at this site. The use of rain barrels as LID controls can convert this into a 9 year event.



**Figure 3.22: Reduction in peak flow with and without LID under different storm events at junction 28 based on subwatershed 36**

### 3.7. Discussion

#### 3.7.1. LID choice

The use of LID practices can increase the return periods of events by more than double. Rain barrels and permeable pavement were simulated based on the cost effectiveness and the area available for LID practices in the study area. Rain barrels are effective and easily maintainable retention and detention devices that are applicable to urban areas (Aad et al. 2010; Damodaram et al. 2010). Among the implemented LID types, rain barrel was noted to have the greatest effect on peak flow and runoff volume reduction. The water collected in the rain barrel can be used to

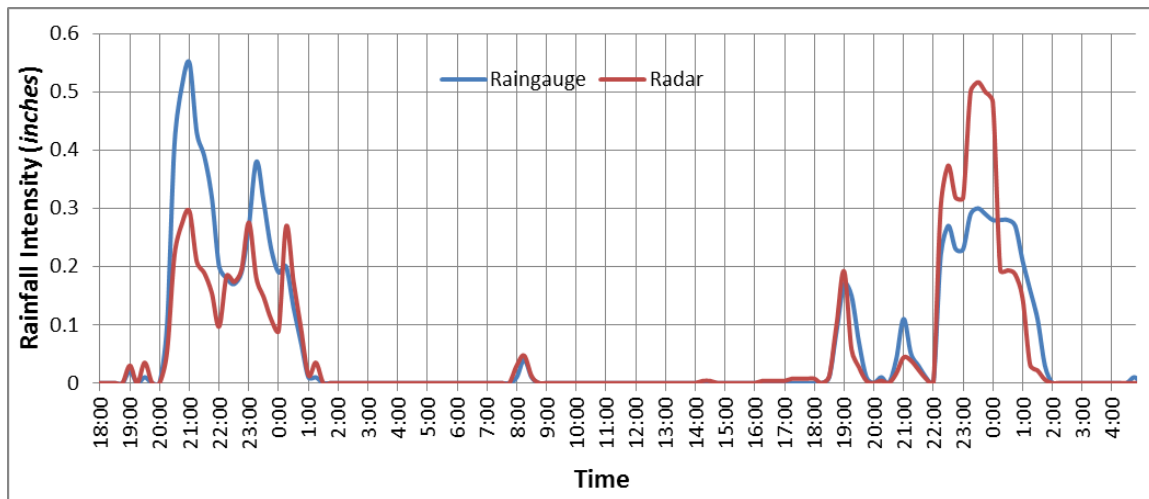
water lawns and gardens, or for other outdoor chores, and rain barrels can also help reduce a homeowner's water bill as watering lawns and gardens, especially the summer months. Rain barrels require less maintenance compared to other LID practices. Rain barrels and cisterns require minimal maintenance. The barrel must be cleaned once a year if debris accumulates. There is no maintenance for preventing mosquito breeding in the tank if the downspout entrance is sealed well. Cost of rain barrel depends on its size and type of material it is made. A single residential rain barrel costs around \$50 for the parts for self-assembly and \$200 assembled. Cisterns costs can start at around \$1500 (University of Florida, 2008). Rain barrels or cisterns can be located above ground, underground, or inside building basements.

Note that bioretentions can serve similar purposes as rain barrels/cisterns. They are also visually more attractive choices. However, when bioretentions are integrated into a development site, the designer must consider site conditions and constraints, proposed land uses, soil types, stormwater pollutants, soil moisture conditions, proper drainage, groundwater recharge, and overflows. Bioretention facilities require many maintenance efforts such as weeding of unwanted plant materials, watering is necessary if plants wilt during hot days, soil fertility, mulching, standing water problems, trash and debris carried by runoff flowing (County 2007).

### **3.7.2. Uncertainty in Rainfall Data**

The simulations in this research were conducted by a model calibrated using field data. Nevertheless, there are many uncertainties varying from model input parameters to input to measured stage data. Rainfall data from radar-based estimates were compared to our rain gauge data during two big events (16-17 May, 2015) and are shown in Figure 3.23. During the rain event on 05/16/2015, the simulated water depth based on our rain gauge rainfall data is greater

than the simulated water depth from radar-based precipitation data. On the other hand, during the rain event on 05/17/2015, the simulated water depth from radar-based precipitation data is greater than the one simulated with the rain gauge data. Therefore, there are uncertainties in rainfall data. When the observed maximum water depths were compared to the simulated ones, the model underestimated depths in large events. During large storms, there could be another water source flowing into the TSBW. The stormwater drainage system of TSBW was not considered because of lack of information when the SWMM was calibrated. During the study period, there was almost no water at some sites in the stream unless it is large rain event. Many times, although there was some water flowing at sites 4 and 5 during rainless periods, no water was seen at site 3, which is downstream of sites 4 and 5. Therefore, it is assumed that water is leaking to the ground from the concrete channel at some locations, and potentially showing up somewhere else.



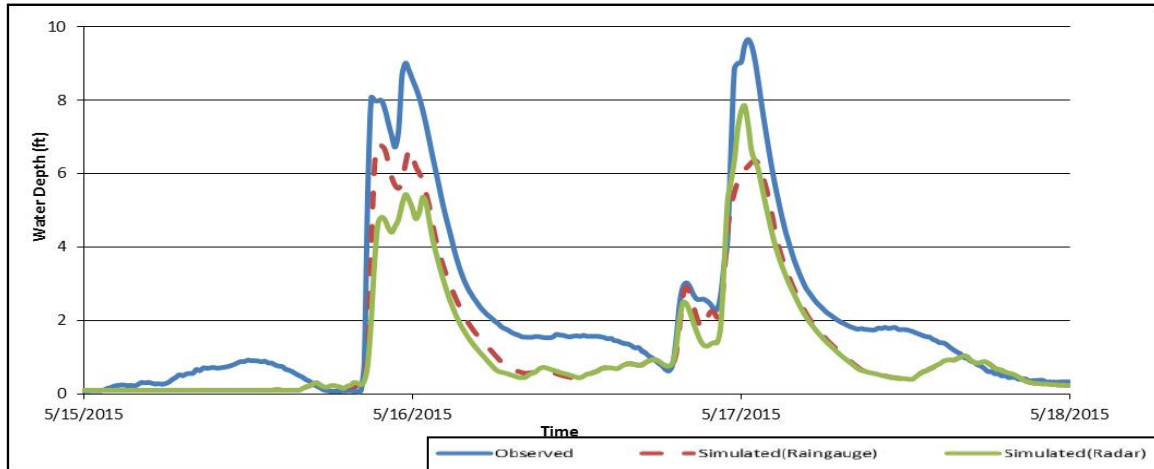


**Figure 3. 23. A comparison between rainfall data from radar with rain gauge data**

### 3.7.3. Clogged Channels

During the field visits, waterways clogged by debris at multiple sites were observed. This clogging caused water to back up, leading to local flooding of some roads and the backyards of houses (Figure 3.24). The Storm Water Management Model (SWMM) cannot account for clogged channel conditions since this situation is unpredictable, and SWMM does not include trash deposits in channels as a model process (again highly unpredictable).



**Figure 3. 24. The channel being clogged by vegetation and trash at site 5**

### **3.7.4. Junction 20 and 28 Capacity**

J20 and J28 are the most problematic junctions in the system based on the analysis presented in section 3.3. The problem with junction 28 is its low surcharge depth and low maximum depth in comparison to other junctions in the system. The suggestion for improving the capacity of these junctions is to change their surcharge depth and maximum depth to a higher value. This can be done by changing their physical structure or lowering the level of the storage even though LID principles promote storing and reducing the runoff.

### **3.7.5. Education**

One of the most effective ways of mitigating the flooding issue in urban areas and protecting sensitive areas is education. It is important to inform property owners and residents for flooding risks. As mentioned in section 2.1, channels clogged by vegetation and trash caused water to back up, leading to some local flooding issues in the TSB watershed. After interviewing one Prichard resident who lives next to site 5 (Figure 2.8), he said he did not see the water back-up problem anymore after the city cleaned the debris from the channel (Figure 2.6). During the field visits, car tires and house items were also observed along the stream (Figure 3.25). The mitigating efforts for flooding in this case can be easily done if locals dispose of the trash properly instead of throwing into the stream.



**Figure 3. 25. Debris along the Toulmins Spring Branch**

## 4. CONCLUSIONS

A direct consequence of urban and suburban development is potential land cover change, which can alter the natural flow regime by increasing runoff and decreasing infiltration. Common results are increased magnitude, frequency, duration, and timing (predictability) which can lead to flooding and significant flood damages. Historically, the peak flow has been managed by traditional stormwater management through the use of detention ponds. However, the increased runoff volume was not mainly considered to reduce with conventional stormwater management. Low Impact Development (LID) is suggested as the solution to problems associated with conventional stormwater management.

LID is a land planning and stormwater management technique that minimizes stormwater runoff through natural resource based site design and seeks to control runoff as near to the source of stormwater as possible. The main goal of this study was to investigate the flooding issue at the Toulmins Spring Branch Watershed (TSBW) and evaluate various LID options for flood mitigation. Major findings of this study are as follows.

- i. Although study period was a very wet period, no widespread flooding was observed based on water stage data collected from 5 different locations. Flooding related complains appear to be highly local and related to lack of maintenance of the waterways.
- ii. The SWMM model performed well at the TSBW in predicting water levels in spite of the lack of knowledge of the stormwater drainage system. Neither the city nor the county had a map of the stormwater drainage system. The infrastructure looked very old. Thus, how well the drainage system functions is questionable.

iii. Among various LID options, rain barrels and cisterns were identified as the best choice for this area because of their effectiveness in reducing peak flow and runoff as well as their low costs. Further, they occupy very small areas and require very little maintenance.

Rain barrels and permeable pavements were simulated as LID practices in TSBW. It was estimated that suggested LID practices, under rainfalls corresponding to return period 2, 5, 10, 25, 50, and 100-year storm, can decrease peak flow by 18-25%, depth by 5-16%, and runoff volume by 1-24% compared to the existing conditions where no LIDs exist. These results show that LID is worthy of consideration for urban flood control not only in future development but also in already developed neighborhoods as a stormwater management planning tool.

Flood inundation mapping is influenced by many factors such as the quality of terrain data (DEM, Light Detection and Ranging (LiDAR)), the cross-sectional configuration, and the use of a one (1-D) or two-dimensional (2-D) hydraulic model (Mohammed and Qasim 2012). The 1-D version of HEC-RAS was employed in this study. HEC-RAS is a widely accepted model and predicts average velocity in cross section and water surface elevation. On the other hand, it is very challenging to model in 1-D the ineffective flow areas, losses from channel bends, and overtopping levee sections from systems. Two-dimensional models can be used for this research to predict depth-averaged two-dimensional velocity and water surface elevation. They combine channel bathymetry + LiDAR (floodplains) + Surface Roughness into a velocity field. Therefore, more accurate floodplain maps could have been generated (which was not the real focus of this study).

Water level data collected by pressure transducers were used to calibrate the SWMM model. Although some discharge measurements were taken, it was too few for use in model

calibration. A better model could have been produced if there was flow data in addition to depth data.

## 5. FUTURE WORK

Toulmins Spring Branch has been identified as being impaired by pathogens (fecal coliform) by the State of Alabama. The §303(d) listing was originally reported on Alabama's 2004 List of Impaired Waters. The sources of the impairment are listed as urban runoff and storm sewers. USGS collected data on Toulmins Spring Branch at Graham Avenue (#0247101550) in 2000 and 2001. Of seven samples collected over that period, four exceeded the single sample maximum criterion of 2,000 colonies/100 mL (ADEM 2009).

During the study period, water samples were taken for *Escherichia coli* (*E.coli*) twice after the rain events. The results are shown in Table 5.1.

**Table 5.1. E.coli results at 5 sites**

Date	Site 1	Site 2	Site 3	Site 4	Site 5
11/23/2014	152 MPN/100mL	4730 MPN/100mL	1120 MPN/100mL	10800 MPN/100mL	20800 MPN/100mL
2/15/2016	360 <i>E.coli</i> colonies /100mL	2100 <i>E.coli</i> colonies /100mL	3260 <i>E.coli</i> colonies /100mL	4330 <i>E.coli</i> colonies /100mL	2760 <i>E.coli</i> colonies /100mL

Table 5.2 shows the Alabama Water Watch (AWW) standards summarizing relatively safe and unsafe levels of *E.coli* in water. Note that the value of 200 *E. coli* /100mL level defining safe versus unsafe water corresponds closely with EPA's and ADEM's criteria of 235 *E. coli* /100 mL Statistical Threshold Value (based on a single sampling event) (Bacteriological monitoring 2016).

**Table 5.1: The Alabama Water Watch (AWW) E.coli in water**

	<b>Number of <i>E. coli</i> per 100 mL</b>
Safe for human contact	<200
Risk for human illness	200-600
Unsafe for human contact	>600

Based on these limited data all the sites, except Site 1 (most downstream), are highly unsafe for humans. It would be worth following up this study with another one to trace the sources of *E.coli*.

## REFERENCES

- Aad, M. P. A., Suidan, M. T., and Shuster, W. D. (2010). "Modeling techniques of best management practices: Rain barrels and rain gardens using EPA SWMM-5." *J. Hydrol. Eng.*, 10.1061/(ASCE)HE.1943-5584.0000136, 434–443.
- Abbott, C. L., & Comino- Mateos, L. (2003). IN- SITU HYDRAULIC PERFORMANCE OF A PERMEABLE PAVEMENT SUSTAINABLE URBAN DRAINAGE SYSTEM. *Water and Environment Journal*, 17(3), 187-190.
- Abi Aad, M. P., Suidan, M. T., & Shuster, W. D. (2009). Modeling techniques of best management practices: rain barrels and rain gardens using EPA SWMM-5. *Journal of Hydrologic Engineering*, 15(6), 434-443.
- Alabama Department of Environmental Management (ADEM). (2009). Final Total Maximum Daily Load (TMDL) for Toulmins Spring Branch Assessment Unit ID # AL03160204-0504-300 Pathogens (fecal coliform). Retrieved from <http://adem.alabama.gov/programs/water/wquality/tmdl/FinalToulminsSpringBranchPathogensTMDL.pdf>.
- Ahiablame, L. M., Engel, B. A., & Chaubey, I. (2013). Effectiveness of low impact development practices in two urbanized watersheds: Retrofitting with rain barrel/cistern and porous pavement. *Journal of environmental management*, 119, 151-161.
- Alfredo, K., Montaldo, F., & Goldstein, A. (2009). Observed and modeled performances of prototype green roof test plots subjected to simulated low-and high-intensity precipitations in a laboratory experiment. *Journal of Hydrologic Engineering*, 15(6), 444-457.
- American Society of Civil Engineers. (2000). Design and Construction of Urban Stormwater Management Systems. Manuals And Reports on Engineering Practice No. 77. ISBN 978-0-87262-855-7.
- Andoh, R. Y. G., & Declerck, C. (1997). A cost effective approach to stormwater management? Source control and distributed storage. *Water science and Technology*, 36(8), 307-311.

- Bacteriological Monitoring. (n.d.). Retrieved May 26, 2016, from  
<http://www.alabamawaterwatch.org/resources/frequently-asked-questions/bacteriological-monitoring/>.
- Boyle, D. P., Gupta, H. V., & Sorooshian, S. (2000). Toward improved calibration of hydrologic models: Combining the strengths of manual and automatic methods. *Water Resources Research*, 36(12), 3663-3674.
- Choi, K. S., & Ball, J. E. (2002). Parameter estimation for urban runoff modelling. *Urban water*, 4(1), 31-41.
- Clary, J., Jones, J., & Urbonas, B. (2009). Challenges in Attaining Recreational Stream Standards for Bacteria: Setting Realistic Expectations for Management Policies and BMPs. Paper presented at the World Environmental and Water Resources Congress 2009: Great Rivers.
- Coffman, L. S. (2009). Low Impact Development Technology Course. April 2009 Aurora, CO
- County, P. G. S. (2007). Bioretention manual. Environmental Services Division Department of Environmental Resources. The Prince George's County, Maryland. Watershed Protection Branch, Landover, MD. Available at:  
[http://www.ct.gov/deep/lib/deep/p2/raingardens/bioretention\\_manual\\_2009\\_version.pdf](http://www.ct.gov/deep/lib/deep/p2/raingardens/bioretention_manual_2009_version.pdf)  
 (accessed 5/18/2016).
- Cook, A., & Merwade, V. (2009). Effect of topographic data, geometric configuration and modeling approach on flood inundation mapping. *Journal of Hydrology*, 377(1), 131-142.
- Cronshey, R. G., Roberts, R. T., & Miller, N. (1985, August). Urban hydrology for small watersheds (TR-55 Rev.). In *Hydraulics and Hydrology in the Small Computer Age* (pp. 1268-1273). ASCE.
- Damodaram, C. et al. (2010). "Simulation of combined best management practices and low impact development for sustainable stormwater management." *J. Am. Water Resour. Assoc.*, 46(5), 907-918.
- Davis, A. P., Shokouhian, M., Sharma, H., Minami, C., & Winogradoff, D. (2003). Water quality improvement through bioretention: Lead, copper, and zinc removal. *Water Environment Research*, 73-82.

- Damodaram, C., Giacomoni, M. H., Prakash Khedun, C., Holmes, H., Ryan, A., Saour, W., & Zechman, E. M. (2010). Simulation of combined best management practices and low impact development for sustainable stormwater management1.
- Davis, A. P. (2007). Field performance of bioretention: Water quality. *Environmental Engineering Science*, 24(8), 1048-1064.
- Dietz, M. E., and Clausen, J. C. (2006). Saturation to improve pollutant retention in a rain garden. *Environ. Sci. Technol.*, 40, 1335–1340.
- Dietz, M. E., & Clausen, J. C. (2006). Saturation to improve pollutant retention in a rain garden. *Environmental Science & Technology*, 40(4), 1335-1340.
- Dilley, M. (2005). Natural disaster hotspots: a global risk analysis (Vol. 5). World Bank Publications.
- Di Pierro, F., Khu, S. T., & Savi, D. (2006). From single-objective to multiple-objective multiple-rainfall events automatic calibration of urban storm water runoff models using genetic algorithms. *Water Science & Technology*, 54(6-7), 57-64.
- Dotto, C. B. S., Kleidorfer, M., Deletic, A., Rauch, W., & McCarthy, D. T. (2014). Impacts of measured data uncertainty on urban stormwater models. *Journal of Hydrology*, 508, 28-42.
- Douglas, I., & Alam, K. (2006). Climate change, urban flooding and the rights of the urban poor in Africa: Key findings from six African cities. Action Aid, London, 6.
- Dreelin, E. A., Fowler, L., & Carroll, C. R. (2006). A test of porous pavement effectiveness on clay soils during natural storm events. *Water Research*, 40(4), 799-805.
- Earles, A., Rapp, D., Clary, J., & Lopitz, J. (2009). Breaking down the Barriers to Low Impact Development in Colorado. Paper presented at the World Environmental and Water Resources Congress 2009: Great Rivers.
- EPA (2000). Low Impact Development - A Literature Review. U.S. Environmental Protection Agency, Washington, DC
- EPA (2007). Reducing Stormwater Costs through Low Impact Development (LID) Strategies and Practices. U.S. Environmental Protection Agency, Washington, DC.
- Engineers, U. A. C. O. (2002). HEC-GeoRAS. User's Manual. Davis. US Army Corps of Engineers.

- Fassman, E. A., & Blackbourn, S. (2010). Urban runoff mitigation by a permeable pavement system over impermeable soils. *Journal of Hydrologic Engineering*, 15(6), 475-485.
- Fang, T., & Ball, J. E. (2007). Evaluation of spatially variable control parameters in a complex catchment modelling system: a genetic algorithm application. *Journal of Hydroinformatics*, 9(3), 163-173.
- FEMA, 2008, Multi-year Flood Hazard Identification Plan, version 3, 24 pp.; available online at <<http://www.fema.gov/library/viewRecord.do?id=3276>>.
- Ferguson, B. K. (2005). Porous Pavements. Boca Raton, FL: CRC Press.
- Feyen, L., Vrugt, J. A., Nualláin, B. Ó., van der Knijff, J., & De Roo, A. (2007). Parameter optimisation and uncertainty assessment for large-scale streamflow simulation with the LISFLOOD model. *Journal of Hydrology*, 332(3), 276-289.
- University of Florida (2010). Report prepared for IFAS Extension. Florida field guide to Low Impact Development. Available at : [http://buildgreen.ufl.edu/Fact\\_%20sheet\\_Cisterns\\_Rain\\_Buckets.pdf](http://buildgreen.ufl.edu/Fact_%20sheet_Cisterns_Rain_Buckets.pdf) (accesses 5/18/2016).
- Hollis, G. E. (1977). WATER YIELD CHANGES AFTER THE URBANIZATION OF THE CANON'S BROOK CATCHMENT, HARLOW, ENGLAND/Changements de l'apport d'eau à la suite de l'urbanisation du bassin versant de 'Canon's Brook' à Harlow, en Angleterre. *Hydrological Sciences Journal*, 22(1), 61-75.
- Houle, K. M. (2008). Winter Performance Assessment of Permeable Pavements. University of New Hampshire Stormwater Center, University of New Hampshire.
- Hunt, W. F., Smith, J. T., Jadlocki, S. J., Hathaway, J. M., & Eubanks, P. R. (2008). Pollutant removal and peak flow mitigation by a bioretention cell in urban Charlotte, NC. *Journal of Environmental Engineering*, 134(5), 403-408.
- Huong, H. T. L., & Pathirana, A. (2013). Urbanization and climate change impacts on future urban flooding in Can Tho city, Vietnam. *Hydrology and Earth System Sciences*, 17(1), 379-394.
- Gupta, H. V., Sorooshian, S., & Yapo, P. O. (1999). Status of automatic calibration for hydrologic models: Comparison with multilevel expert calibration. *Journal of Hydrologic Engineering*, 4(2), 135-143.

- Jennings, D. B., & Jarnagin, S. T. (2002). Changes in anthropogenic impervious surfaces, precipitation and daily streamflow discharge: A historical perspective in a midAtlantic subwatershed. *Landscape Ecology*, 17, 471–489.
- Jia, H., Lu, Y., Shaw, L. Y., & Chen, Y. (2012). Planning of LID–BMPs for urban runoff control: The case of Beijing Olympic Village. *Separation and Purification Technology*, 84, 112-119.
- Kalin, L., & Hantush, M. M. (2009). An auxiliary method to reduce potential adverse impacts of projected land developments: Subwatershed prioritization. *Environmental management*, 43(2), 311-325.
- Lazaro, T. R. (1990). Urban hidrology. A multidisciplinary perspective (No. 551.48091732 L431). Technomic Publishing.
- Lee, J. M., Hyun, K. H., and Choi, JS. (2013). “Analysis of the impact of low impact development on runoff from a new district in Korea.” *Water Sci Technol*. 2013;68(6):1315-21. doi: 10.2166/wst.2013.346.
- Lee, J. M., Hyun, K. H., Choi, J. S., Yoon, Y. J., and Geronimo, F. K. F. (2012). “Flood reduction analysis on watershed of LID design demonstration district using SWMM5.” *Desalination and Water Treatment.*, 10.1080/19443994.2012.664377, Volume 38, Issue 1-3, 2012, pages 255-261.
- Lee, S. B., Yoon, C. G., Jung, K. W., & Hwang, H. S. (2010). Comparative evaluation of runoff and water quality using HSPF and SWMM. *Water Science & Technology*, 62(6).
- Leung, J., 2008. Rainwater Harvesting 101. Report prepared for GrowNYC. August. Available at: <http://www.grownyc.org/files/osg/RWH.how.to.pdf> (accessed 18.12.12).
- Leopold, L. B. (1968). Hydrology for urban land planning: A guidebook on the hydrologic effects of urban land use (p. 18). Washington, DC, USA: US Government Printing Office.
- Liao, Z. L., He, Y., Huang, F., Wang, S., & Li, H. Z. (2013). Analysis on LID for highly urbanized areas' waterlogging control: demonstrated on the example of Caohejing in Shanghai. *Water Science & Technology*, 68(12).
- Liong, S. Y., Chan, W. T., & Lum, L. H. (1991). Knowledge-based system for SWMM runoff component calibration. *Journal of Water Resources Planning and Management*, 117(5), 507-524.

- McCuen, R. H. (2002). Modeling hydrologic change: statistical methods. CRC press.
- Milly, P. C. D., Julio, B., Malin, F., Robert, M., Zbigniew, W., Dennis, P., & Ronald, J. (2007). Stationarity is dead. *Ground Water News & Views*, 4(1), 6-8.
- Mobile County Revenue Commission, downloaded from County GIS, August 2013.
- Mohammed, J. R., & Qasim, J. M. (2012). Comparison of one-dimensional HEC-RAS with twodimensional ADH for flow over trapezoidal profile weirs. *Caspian Journal of Applied Sciences Research*, 1(6), 1-12.
- Montalto, F., Behr, C., Alfredo, K., Wolf, M., Arye, M., & Walsh, M. (2007). Rapid assessment of the cost-effectiveness of low impact development for CSO control. *Landscape and urban planning*, 82(3), 117-131.
- Moscrip, A. L., & Montgomery, D. R. (1997). URBANIZATION, FLOOD FREQUENCY, AND SALMON ABUNDANCE IN PUGET LOWLAND STREAMS1.
- Nash, J. E., & Sutcliffe, J. V. (1970). River flow forecasting through conceptual models part I— A discussion of principles. *Journal of hydrology*, 10(3), 282-290.
- National Aeronautics and Space Administration, Downloaded 2008
- Natural Resources Conservation Service. (1980). Soil survey of Mobile County, ALABAMA. available in:  
[http://www.nrcs.usda.gov/Internet/FSE\\_MANUSCRIPTS/alabama/AL097/0/mobile.pdf](http://www.nrcs.usda.gov/Internet/FSE_MANUSCRIPTS/alabama/AL097/0/mobile.pdf)
- NOAA,2014.United States Flood Loss Report. Available at:  
<http://www.nws.noaa.gov/hic/summaries/WY2014.pdf>.
- Neitsch, S. L., Arnold, J. G., Kiniry, J. R., & Williams, J. R. (2011). Soil and water assessment tool theoretical documentation version 2009. Texas Water Resources Institute.
- Pratt, C. J., Newman, A. P., & Bond, P. C. (1999). Mineral oil bio-degradation within a permeable pavement: long term observations. *Water Science and Technology*, 39(2), 103-109.
- Prince George's County (2000a). Low-Impact Development an Integrated Design Approach. Largo, MD: Prince George's County, Maryland.  
<http://www.epa.gov/owow/nps/lid/lidnatl.pdf>.

Prince George's County (2000b). Low-Impact Development Hydrologic Analysis Companion Document to the Low-Impact Development Design Strategies. Largo, MD.: Prince George's County, Maryland.

Palhegyi, G. E. (2009). Designing storm-water controls to promote sustainable ecosystems: science and application. *Journal of Hydrologic Engineering*, 15(6), 504-511.

Pandey, D. N., Gupta, A. K., & Anderson, D. M. (2003). Rainwater harvesting as an adaptation to climate change. *Current science*, 85(1), 46-59.

Qin, H. P., Li, Z. X., & Fu, G. (2013). The effects of low impact development on urban flooding under different rainfall characteristics. *Journal of environmental management*, 129, 577-585.

Rawls, W. J., Brakensiek, D. L., & Saxton, K. E. (1982). Estimation of soil water properties. *Transactions of the ASAE*, 25(5), 1316-1320.

Rivas, I., & Roesner, L. A. (2009). Design and Implementation of Optimized Hydrologic Unit Watersheds for Rainfall-Runoff Modeling. In World Environmental and Water Resources Congress 2009@ sGreat Rivers (pp. 6347-6356). ASCE.

Roebuck, R.M., 2007. An investigation into the whole life cost implications of using rainwater harvesting systems for non-potable applications in new-build developments in the UK. PhD dissertation. University of Bradford, West Yorkshire, UK.

Rose, S., & Peters, N. E. (2001). Effects of urbanization on streamflow in the Atlanta area (Georgia, USA): a comparative hydrological approach. *Hydrological Processes*, 15(8), 1441-1457.

Rossman, L. A., 2006. Storm Water Management Model Quality Assurance Report: Dynamic Wave Flow Routing. Environmental Protection Agency of United States of America.

Rossman, L. A. (2010). Storm water management model user's manual, version 5.0 (p. 276). Cincinnati: National Risk Management Research Laboratory, Office of Research and Development, US Environmental Protection Agency.

Rossman, L. A., 2015. Stormwater Management Model user's manual version 5.1. Environmental Protection Agency of United States of America.

Saghafian, B., & Khosroshahi, M. (2005). Unit response approach for priority determination of flood source areas. *Journal of hydrologic engineering*, 10(4), 270-277.

- Scholz, M., & Grabowiecki, P. (2007). Review of permeable pavement systems. *Building and Environment*, 42(11), 3830-3836.
- Shaw EM (1994) Hydrology in practice, 3rd edn. Chapman & Hall, London, p 569
- Siddiqui, Q. T. M., Hashmi, H. N., & Ghumman, A. R. (2011). Flood inundation modeling for a watershed in the pothowar region of Pakistan. *Arabian Journal for Science and Engineering*, 36(7), 1203-1220.
- Simpson, Matthew, G. (2010). Low Impact Development Modeling To Manage Urban Storm Water Runoff And Restore Predevelopment Site Hydrology. Master's thesis, Colorado State University Fort Collins, Colorado, Summer 2010
- Smith, A. B., & Katz, R. W. (2013). US billion-dollar weather and climate disasters: data sources, trends, accuracy and biases. *Natural hazards*, 67(2), 387-410.
- Southeast Regional Climate Center <http://www.sercc.com/cgi-bin/sercc/cliMAIN.pl?al5483>; Daily Temperature Averages and Extremes for POR 1930-1965; 2013
- Stahre, P. (2008). Blue-Green Fingerprints in the City of Malmö, Sweden. Malmö, Sweden: VA SYD.
- Sun, N., Hall, M., Hong, B., & Zhang, L. (2012). Impact of SWMM catchment discretization: case study in Syracuse, New York. *Journal of Hydrologic Engineering*, 19(1), 223-234.
- Sun, N., Hong, B., & Hall, M. (2014). Assessment of the SWMM model uncertainties within the generalized likelihood uncertainty estimation (GLUE) framework for a high-resolution urban sewershed. *Hydrological Processes*, 28(6), 3018-3034.
- The National Academies Press, 2009.
- US Geological Survey, National Hydrologic Database, Downloaded April 2013.
- Zahmatkesh, Z., Burian, S. J., Karamouz, M., Tavakol-Davani, H., & Goharian, E. (2014). Low-impact development practices to mitigate climate change effects on urban stormwater runoff: Case study of New York City. *Journal of Irrigation and Drainage Engineering*, 141(1), 04014043.
- Waananen, A. O. (1969). Effects of watershed changes on streamflow. *Urban effects on water yield*, 169-182.
- Wang, J. L., Che, W., & Yi, H. X. (2009). Low Impact Development for Urban Stormwater and Flood Control and Utilization [J]. *China Water & Wastewater*, 14, 003.
- Weather;<http://www.weather.com/outlook/travel/vacationplanner/wxclimatology/month>

ly/36603; The Weather Channel Monthly Averages (temperatures) for Mobile, AL 36603, 2013.

WeatherBill; [http://en.wikipedia.org/wiki/Mobile,\\_Alabama](http://en.wikipedia.org/wiki/Mobile,_Alabama); Climate, 2007.